Role of Secretogranin VII (VGF) in Regulated Exocytosis in Rat Pheochromocytoma Cells

Submitted to

National Brain Research Centre, Manesar

In Partial Fulfilment of the Requirements for the Degree of Master of Science in Neuroscience

Sanchari Banerjee
M.Sc. Neuroscience, Final Year
June, 2025

National Brain Research Centre
NH-8, near NSG Campus Manesar,
Haryana, 122052

CERTIFICATE

This is to certify that the dissertation report titled '**Role of Secretogranin VII (VGF) in Regulated Exocytosis in Rat Pheochromocytoma Cells**' is the result of work carried out by **Sanchari Banerjee** in the **Division of Cellular and Molecular Neuroscience**, National Brain Research Centre, Manesar, Haryana, India, for partial fulfilment of requirements for the M.Sc. Degree.

The work presented herein is original and has not been submitted previously for the award of any degree or diploma to the **National Brain Research Centre (Deemed to be University)** or to any other University. This work is based on the guidelines of the **National Brain Research Centre (Deemed to be University)** and is a record of the candidate's efforts.

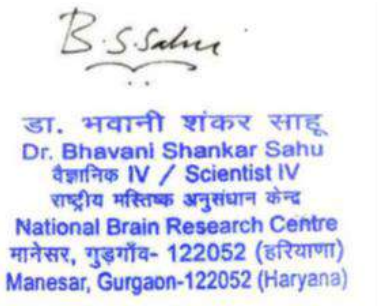
डा. भवानी शंकर साहू
Dr. Bhavani Shankar Sahu
वैज्ञानिक IV / Scientist IV
राष्ट्रीय मस्तिष्क अनुसंधान केन्द्र
National Brain Research Centre
मानेसर, गुड़गाँव- 122052 (हरियाणा)
Manesar, Gurgaon-122052 (Haryana)

Dr. Bhavani Shankar Sahu
(Supervisor)

Dr. Sagar Sengupta
(Director)

Place: Manesar
Date: June 2025

DECLARATION BY CANDIDATE

I, Sanchari Banerjee, declare that the work presented in the dissertation report titled '**Role of Secretogranin VII (VGF) in Regulated Exocytosis in Rat Pheochromocytoma Cells**' was carried out by me under the guidance of **Dr. Bhavani Shankar Sahu, Division of Cellular and Molecular Neuroscience,** National Brain Research Centre (Deemed to be University), Manesar, Haryana, India.

I declare that no part of the thesis contains any plagiarised material. Any previously published or other material sourced from anywhere else has been appropriately attributed to the source.

I also declare that no part of this thesis has been previously submitted to earn any degree/diploma from the **National Brain Research Centre (Deemed to be University)** or any other university.

Place: Manesar
Date: June, 2025

Sanchari Banerjee

Sanchari Banerjee

Acknowledgements

First and foremost, I express my deepest gratitude to the **Almighty** for giving me the strength, patience, and resilience to complete this journey. In moments of doubt and difficulty, it was my faith that grounded me and guided me forward.

I would like to express my humble gratitude to **DBT-NBRC** for providing me with a stipend and funding my project to carry out the study comfortably. I want to thank my supervisor, **Dr. Bhavani Shankar Sahu**, whose guidance and support has led to the successful completion of this project. I am highly indebted to my mentor, **Shashank Saxena**, who showed keen interest at every stage of my project and helped me conceptualise my experiments. It has been an immense privilege to work under his mentorship. My deep sense of gratitude to **Dr. Sushma Dagar** and **Krittika Biswas** for being pillars of strength, laughter, and comfort. Your presence created an environment that was both intellectually stimulating and personally comforting. Here's to **Chandramouli Mukherjee** and **Palki Chauksey**, for supporting and contributing to all the madness that came along with long lab hours and last-minute panic. Your friendship and humour made the chaos manageable and memorable. I also extend my thanks to **Dr. Puyam Milan Meitei, Mohima Mukherjee, Tamanna Saini, Shreya Kumari, Nikhitha Nair Upasna Mohapatra, Sourav Chatterjee, Yasoswini Khatua** and **Ankita Roy** for being kind and collaborative lab mates. I would also like to thank **Mr. P. Manish, Mr. Mahendra Singh,** and **Mr. Ankit Sharma** for their efforts in maintaining the available lab equipment.

I am also thankful to my batchmates, **Aarya, Aashi, Atharva, Austin, Gauri, Ritu,** and **Vibha**, for their encouragement and support during the tough times.

Finally, I extend my deepest and most heartfelt gratitude to my **Parents** and **Family** for their unconditional love and blessings throughout my academic career and for believing in me and my work. Their silent sacrifices have been the wind beneath my wings, helping me soar even when I doubted myself. I would also like to thank my best friends, **Anwesha Haldar** and **Dr. Arjya Mukherjee**, for giving me immense love and mental peace. Thank you for being my constant companions, cheering me on, lifting me up, and never letting me lose sight of my potential. I am extremely grateful to **Anwesha Dutta, Arhana Bhowmik, Shrabona Mukherjee, Twanni Das, Abhipsa Mondal** and **Rajit Dutta** for effortlessly being there and never giving up. Thanks for being like my rays of sunshine when my clouds were grey. Lastly, special thanks to my roommate **Pawanpreet Kaur Saini** for her constant support. Your quiet strength, comforting presence, and unspoken support have meant more than words can express. You've been my sounding board, my safe space, and a true friend in every sense. This thesis is not just a culmination of academic effort, but a reflection of the people who shaped it alongside me. This project is dedicated to my **Maa**. Her endless sacrifices, boundless love, and unwavering belief in me has shaped me to who I am today. Her strength runs through my veins, and her dreams live in my accomplishments. Though words will always fall short, I hope this achievement makes her proud, as I carry her love and legacy forward through every challenge and triumph.

Abstract

Secretogranin VII, also known as VGF, is a member of the Granin family of acidic secretory proteins[1] are predominantly stored in dense core vesicles (DCVs) and play key roles in the regulated secretory pathway (RSP) of neurons and neuroendocrine cells[2,3]. Although VGF has been implicated in multiple physiological processes, including energy homeostasis, synaptic plasticity, and neuroendocrine signalling[4,5], its mechanistic role in vesicle trafficking and secretion remains poorly defined.

In this study, we aim to elucidate the role of VGF in regulated secretion using the rat pheochromocytoma-derived PC12 cell line, a well-established model for studying neurosecretory processes[6]. We generated VGF knockout (KO) PC12 cells using the CRISPR-Cas9 system[7]. Functional analysis revealed that VGF deficiency resulted in impaired stimulus-coupled secretion, as assessed by potassium-induced depolarisation and live-cell imaging using NPY-pHlourin, a DCV cargo reporter. Importantly, constitutive secretion remained unaltered in the absence of VGF, indicating that the secretory impairment was specific to the RSP. Overexpression of VGF into KO cells via transient transfection partially rescued the impairment of exocytosis, further validating the specificity of the observed defects. To assess whether the impairment extended beyond DCVs, we performed live imaging with synaptophysin-pHlourin, a reporter of synaptic-like vesicles (SLVs), and observed no significant difference between WT and KO cells, suggesting that VGF is specifically required for DCV-mediated exocytosis. STED microscopy using Secretogranin II staining revealed no significant change in the overall number of vesicles per cell between WT and KO conditions. However, vesicle size distribution analysis indicated an accumulation of smaller vesicles (<150 nm) in KO cells, suggesting a defect in vesicle maturation[8]. To assess the nature of exocytotic impairment, dextran uptake assays were performed to differentiate between kiss-and-run and full fusion modes of secretion. While the uptake of 10 kDa dextran (kiss-and-run) was unaffected, KO cells showed significantly reduced uptake of 40 kDa dextran, indicating a specific impairment in full fusion exocytosis. Furthermore, the functionality of the Endolysosomal pathway was assessed by tracing the clearance of 10 kDa dextran. KO cells exhibited a delayed clearance of dextran-positive puncta even after a 6-hour chase period, suggesting a defect in post-exocytotic recycling and trafficking via the Endolysosomal system[9].

Taken together, our findings demonstrate that VGF is a critical regulator of dense core vesicle maturation and full fusion exocytosis in PC12 cells and may influence downstream Endolysosomal recycling. This study sheds new light on the mechanistic role of VGF in neurosecretory physiology, opening new avenues for understanding its contribution to vesicle trafficking-related disorders.

Key words: VGF, Dense Core Vesicles, Regulated Secretion, Exocytosis, Endolysosomal trafficking

Table of Contents

1	**Introduction**	**1**
2	**Review of Literature**	**5**
2.1	Membrane Trafficking	5
2.2	The Regulated Secretory Pathway	7
2.3	Dense Core Vesicles	11
2.4	The Granin Family of Proteins	13
2.5	Bioactive Peptides Derived from the Granin Family	15
2.6	Secretogranin VII and Regulated Exocytosis	16
2.7	VGF-Derived Peptides	17
2.8	Role of VGF in various Neuroendocrine systems	18
3	**Materials and Methods**	**21**
3.1	Cell Culture	21
3.2	Generation of VGF KO cells by CRISPR-Cas9 method	21
3.3	Transfections	22
3.4	Mammalian Expression Constructs	23
3.5	Immunoblotting	23
3.6	Immunocytochemistry	24
3.7	Stimulated Emission Depletion (STED) Microscopy	24
3.8	Stimulus-Coupled Secretion Assay	25
3.9	Live Cell Imaging	26
3.10	Constitutive Secretion	26
3.11	Dextran Uptake Assay	27
3.12	Endolysosomal Assay	27
4	**Results**	**29**
4.1	Cloning of CRISPR-Cas9 gRNAs targeting the VGF Gene	29
4.2	Generation and Validation of VGF KO PC12 Cells	31
4.3	Loss of VGF Impairs Regulated Secretion in PC12 Cells	33
4.4	Constitutive Secretion is unaffected in VGF KO cells	35
4.5	Real-time imaging shows compromised DCV Exocytosis	37
4.6	Rescue of VGF shows Partial Restoration of RSP	39
4.7	Release of SLVs is not altered in VGF KO Cells	41
4.8	STED shows altered vesicle distribution in VGF KO Cells	43
4.9	VGF KO impairs Full Fusion Exocytosis	45
4.10	VGF KO suggests disruption in Endolysosomal Trafficking	46
5	**Discussion**	**49**
6	**Concluding Remarks**	**53**
7	**Future Directions**	**54**
8	**References**	**55**

List of Figures

2.1. Schematic depiction of secretory membrane traffic pathways
2.2. Dense Core Vesicles vs Synaptic Vesicles
2.3. Homotypic Membrane Fusion
2.4. Bioactive Peptides from the Granin Family

4.1. Cloning of gRNAs in the PX459 vector
4.2. Generation and Validation of VGF KO PC12 cells
4.3. Loss of VGF impairs RSP in PC12 Cells
4.4. Constitutive Secretion is not affected in VGF KO PC12 Cells
4.5. Real-time imaging shows compromised DCV Exocytosis
4.6. Rescue experiments reveal partial restoration of Regulated Exocytosis
4.7. Release of synaptic-like vesicles is not altered in VGF KO cells
4.8. STED imaging reveals altered vesicle morphology but preserved biogenesis in VGF KO cells
4.9. VGF KO impairs full fusion exocytosis as well as Endolysosomal clearance

5.1. Schematic Representation of impaired RSP in VGF-deficient cells.

Aims and Objectives

Aim: Role of Secretogranin VII (VGF) in Regulated Exocytosis in Rat Pheochromocytoma Cells.

Objectives:

1. Generation of CRISPR-Cas9 Knockouts for VGF in Rat Pheochromocytoma Cells.
2. Evaluate the functional status of regulated exocytosis of DCVs in VGF KO Cells.
3. Investigate the effect on the Constitutive Secretory Pathway in the absence of VGF.
4. Determine the status of VGF KO cells on SLV exocytosis.
5. Characterisation of DCV distribution and size in VGF-deficient cells using Super Resolution Microscopy.
6. Delineate the specific modes of exocytosis that are perturbed upon loss of VGF.

Abbreviations

1. ACTH - Adrenocorticotropic Hormone
2. AD - Alzheimer's disease
3. ALS - Amyotrophic Lateral Sclerosis
4. BCA - Bicinchoninic acid
5. BFA – Brefeldin A
6. BDNF - Brain-derived Neurotrophic Factor
7. BSA - Bovine Serum Albumin
8. CAPS - Calcium Activated Protein for Secretion
9. CSP - Constitutive Secretory Pathway
10. Cg – Chromogranin
11. CgA - Chromogranin A
12. CgB - Chromogranin B
13. CGN - cis Golgi Network
14. CNS - Central Nervous System
15. CSF - Cerebrospinal Fluid
16. DAPI - 4′,6-diamidino-2-phenylindole
17. DCV - Dense Core Vesicle
18. DMEM - Dulbecco's Modified Eagle Medium
19. DMSO - Dimethyl sulfoxide
20. DNA - Deoxyribonucleic Acid
21. ECL - Enhanced Chemiluminescence
22. EGFP - Enhanced Green Fluorescent Protein
23. ER - Endoplasmic Reticulum
24. FBS - Foetal Bovine Serum
25. GAPDH - Glyceraldehyde-3-Phosphate Dehydrogenase
26. GEF - Guanine nucleotide exchange factor
27. GDIs - GDP dissociation inhibitors
28. GDP - Guanosine diphosphate
29. GI - Gastrointestinal
30. GTP - Guanosine triphosphate
31. Guide RNAs - gRNAs
32. HEPES - 4-(2-hydroxyethyl)-1- piperazineethanesulfonic acid
33. HRP - Horseradish Peroxidase
34. HS - Horse Serum
35. HSP90 - Heat Shock Protein 90
36. KO - Knockout
37. LDCVs - Large Dense Core Vesicles

38. LTP – Long Term Potentiation
39. NGF - Nerve Growth Factor
40. NPY - Neuropeptide Y
41. NT3 – Neurotrophin 3
42. PA - Phosphatidic acid
43. PAGE - Polyacrylamide Gel Electrophoresis
44. PBS - Phosphate Buffered Saline
45. PC12 - Pheochromocytoma
46. PD - Parkinson's Disease
47. PFA - Paraformaldehyde
48. PLL - Poly-L-Lysine
49. RAB - Ras-associated binding
50. RER – Rough Endoplasmic Reticulum
51. RIPA - Radioimmunoprecipitation assay
52. RNA - Ribonucleic Acid
53. RUSH - Retention Using Selective Hooks
54. Scg - Secretogranin
55. ScgII - Secretogranin II
56. ScgIII - Secretogranin III
57. SCPs - Schwann Cell Precursors
58. SCSA – Stimulus Coupled Secretion Assay
59. SDS - Sodium Dodecyl Sulphate
60. SLV - Synaptic-like Vesicle
61. SLP1 - Synaptotagmin-like Protein 1
62. SNARE - Soluble NSF Attachment Protein Receptor
63. STED – Stimulated Emission Depletion
64. SVs - Synaptic Vesicles
65. TBST - Tris Buffered Saline, with Tween-20
66. TEM – Transmission Electron Microscopy
67. TGN - trans Golgi Network
68. Trk – Tropomysin Receptor Kinase
69. V-ATPases - Vacuolar-type H^+-ATPases
70. WT - Wild Type

Chapter 1
Introduction

Chapter 1

Introduction

The intracellular trafficking and regulated secretion of neuropeptides, hormones, and proteins are essential for the proper functioning of neurons and neuroendocrine cells, allowing for precise temporal and spatial control of intercellular communication[10,11]. These processes are particularly crucial in the nervous and endocrine systems, where signaling molecules must be delivered in a stimulus-dependent manner to maintain homeostasis, synaptic plasticity, and organismal behaviour[12,13].

A specialized class of vesicles known as dense core vesicles (DCVs) mediates the storage and activity-dependent release of neuropeptides and hormones. Unlike synaptic vesicles, which release classical neurotransmitters, DCVs are involved in slower, modulatory signaling and are synthesized in the trans-Golgi network (TGN) before being trafficked to the plasma membrane[14,15]. The regulated secretion of DCVs requires a complex orchestration of vesicle biogenesis, cargo sorting, maturation, trafficking, docking, and fusion, which is tightly controlled by numerous proteins, including SNAREs, granins, Rab GTPases, and adaptor complexes[16,17]. Among these regulatory proteins, the Granin family of acidic secretory proteins has been recognized as a central component of the regulated secretory pathway. This family includes Chromogranins (CgA, CgB) and Secretogranins (ScgII, ScgIII, VGF), which are widely expressed in endocrine and neuroendocrine cells and are packaged into DCVs during their formation[3,18]. Granins not only function as prohormone precursors but also participate in the sorting and condensation of cargo proteins within the vesicles and influence vesicle morphology and stability[18,19].

VGF (non-acronymic), also known as Secretogranin VII, was originally identified as a nerve growth factor (NGF) responsive gene in PC12 cells, a rat pheochromocytoma-derived neuroendocrine cell line[20]. It is selectively expressed in neurons and endocrine tissues and is stored predominantly in DCVs, where it undergoes proteolytic processing to produce bioactive peptides[1,21]. VGF-derived peptides such as TLQP-21 and NERP-1 have been shown to regulate energy balance, mood, nociception, and neurogenesis, linking VGF to a broad range of physiological processes[22-24]. Despite extensive studies

on its physiological relevance, the specific mechanistic role of VGF in the trafficking, maturation, and exocytosis of DCVs remains poorly defined. Emerging evidence suggests that VGF may play a structural or regulatory role in dense core vesicle biology, possibly influencing vesicle size, content, or fusion competency[25,26]. However, direct mechanistic studies elucidating how the absence of VGF affects secretion are limited. Given the importance of understanding molecular regulators of vesicle trafficking and the utility of PC12 cells as a model system for studying regulated secretion, this thesis aims to investigate the role of VGF in neurosecretory processes. Using CRISPR-Cas9 technology to generate VGF KO cell lines, we examine the consequences of VGF loss on dense core vesicle-mediated secretion, vesicle morphology, and exocytosis, thereby shedding light on its potential role in vesicle maturation and Endolysosomal recycling pathways.

Chapter 2
Review of Literature

Chapter 2

Review of Literature

2.1 Membrane Trafficking

Membrane trafficking broadly refers to the movement of cargo either from the intracellular environment to the extracellular space (exocytosis) or from the extracellular space to the intracellular environment (endocytosis)[27]. To comprehend the fundamentals of cellular function and survival, it is crucial to trace the pathways proteins follow within a cell as they perform various roles[28]. Replication and transcription occur in the nucleus, after which mRNA exits to be translated into proteins by ribosomes on the Endoplasmic Reticulum (ER) membrane[29]. Specific signal sequences (Signal Recognition particles) on the peptides target these proteins to the ER, where they undergo post-translational modifications and get sorted into further compartments[30]. The three major destinations for cargo include the Golgi, lysosomes, and the plasma membrane, each of which marks the various underlying cellular mechanisms[31]. These compartments are lined by a unique lipid-protein composition, which restricts the free movement of cargo between them[32]. Hence, trafficking through these organelles is mediated by vesicles coated with special proteins targeting their specific destinations[33,34].

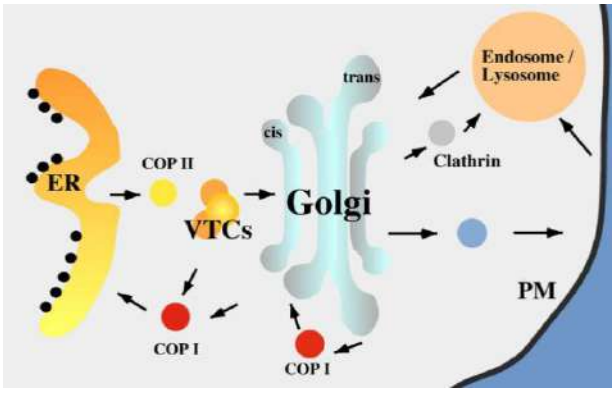

Figure 2.1: Schematic depiction of secretory membrane traffic pathways
Source: Duden R. ER-to-Golgi transport: COP I and COP II function (Review). Mol Membr Biol. 2003 Sep;20(3):197-207

Two classes of such proteins that direct the vectorial transfer of cargo between the ER and the Golgi are COPI and COPII, associated with the ER membrane[35]. COPII-coated vesicles mediate the course from the ER to the Golgi, after which they get recruited back to the same domains in the ER membrane and traffic the next cargo during the COPII budding cycle[36,37]. A strictly regulated machinery composed of v-SNARES ensures that only properly folded proteins are carried from the ER to the Golgi by targeting the fusion of these vesicles with the Golgi membrane[38,39]. This cargo can get packed in these vesicles by bulk flow or through interactions between the cargo membrane receptors and the coat[40]. On the other hand, COPI vesicles carry cargo retrogradely from the Golgi to the ER in a selective fashion similar to the COPII vesicles[41,42]. The KDEL receptor is a membrane protein which recognises ER Chaperones bearing the KDEL motif, like PDI and BiP, targeting the COPI-coated vesicles from the Cis-Golgi to the ER[43,44]. The Golgi apparatus is a collection of cisternae stacked and divided into the Cis-Golgi network (CGN) and the trans-Golgi network (TGN)[45,46]. The proteins enter the Golgi through the Cis face and exit through the Trans face, where proteins are packaged into vesicles to be sent to the lysosomes, cell membrane or the extracellular space[27,47]. Following their synthesis, newly translated proteins undergo a series of post-translational modifications as they transit from the ER and through the Golgi apparatus, or as they become residents in specific compartments of the secretory pathway[31]. These modifications are crucial for protein folding, stability, trafficking, and function, and they enable the targeting of proteins to their respective destinations within the cell. Key post-translational modifications include phosphorylation, N- and O-linked glycosylation, disulfide bond formation, acetylation, lipidation (such as palmitoylation and prenylation), proteolytic cleavage, and sulfation [48,49]. One of the crucial modification proteins undergo in the Golgi is the phosphorylation of oligosaccharides on lysosomal proteins in the CGN and the removal of mannose residues at the TGN[50]. The proteins in the TGN have three fates: degradation in the lysosomes, getting embedded in the plasma membrane forming integral proteins or secretion to the extracellular space either constitutively or upon receiving a stimulus[51].

2.2 The Regulated Secretory Pathway

As the name suggests, Neuroendocrine cells represent the intersection of electrical impulses (neural) and chemical signalling (endocrine) in the body[52]. These cells are primarily located in the adrenal, pituitary and parathyroid glands, as well as in organs such as the gastrointestinal (GI) tract, pancreas and thyroid[53,54]. These cells release hormones and peptides in response to signals from the nervous system which are then transported through the bloodstream to bind with specific receptors on target cells, inducing chemical changes[55,56]. For example, release of epinephrine and norepinephrine (catecholamines) by chromaffin cells in the adrenal medulla[57]. Chromaffin cells originate from neural crest cells and develop from peripheral glial stem cells, known as Schwann Cell Precursors (SCPs)[58]. These precursors migrate along the visceral motor nerve to the developing adrenal gland where they finally detach and differentiate[58,59]. These are the primary neuroendocrine source of adrenaline in the body. Positioned near the presynaptic sympathetic nerves of the sympathetic nervous system, chromaffin cells function similarly to the postsynaptic sympathetic nerves[60]. For example, when acetylcholine from the splanchnic nerve binds to the nicotinic acetylcholine receptors on the adrenal medulla, these cells release hormones such as epinephrine and norepinephrine[61]. One of the most commonly studied neuroendocrine cell model is pheochromocytoma (PC12) cells, derived from rat adrenal medulla[6]. This cell line is also known as a professional secretory model because of its wide utilisation in studying regulated secretion[61]. PC12 cells, a model system derived from rat pheochromocytoma, possess two distinct types of secretory vesicles that participate in membrane trafficking and regulated exocytosis: synaptic-like vesicles (SLVs) and dense-core vesicles (DCVs)[8,62]. SLVs are small, clear vesicles that closely resemble neuronal synaptic vesicles in both size and protein composition. They are primarily involved in the rapid, calcium-dependent release of classical neurotransmitters such as dopamine in response to membrane depolarization, thus mimicking synaptic transmission[63,64]. Synaptic vesicles play a role in membrane trafficking and release neurotransmitters upon membrane depolarisation, facilitating nerve impulse conduction[64]. In contrast, DCVs are larger, electron-dense vesicles that store and secrete neuropeptides, hormones, and granins [15]. Their release typically requires stronger or more prolonged stimulation and plays a role in modulating long-term cellular responses, neuroendocrine signalling, and

plasticity[15,65]. Both SLVs and DCVs contribute to the secretory competence of PC12 cells and serve as valuable tools for studying the mechanisms of regulated exocytosis and vesicle maturation[66]. These secretory vesicles are sorted in the trans-Golgi network, where their maturation is regulated by coat proteins like clathrin[57,67]

The major differences between Dense Core Vesicles and Synaptic Vesicles are listed in the table below:[68].

Figure 2.2

Characteristics	Dense Core Vesicles	Synaptic Vesicles
Morphology & Ultrastructure	Large in size (100-300 nm in diameter) and contain an electron dense core due to their proteinaceous cargo.	Small in size (40-50 nm in diameter) with a relatively clear lumen. They appear as uniform, round vesicles with a thinner membrane.
Biogenesis & Origin	Formed at the Trans-Golgi Network (TGN) and transported along microtubules to distal sites. They undergo maturation during which they concentrate their cargo	Primarily recycled locally at the presynaptic termina; through endocytosis, although some can also be derived from the Golgi in developing neurons.
Cargo & Molecular Composition	Carry neuropeptides, hormones and amines. They also contain processing enzymes like prohormone convertases to process precursor proteins into active peptides.	Contain classical neurotransmitters such as Glutamate, GABA, acetylcholine, dopamine and serotonin. They express specific transporters that load neurotransmitters.
Release Mechanism	They undergo regulated secretion, requiring high frequency stimulation and a sustained Ca^{2+} influx. Their exocytosis occurs away from synapses, at dendrites, axons or the soma and is slower than synaptic vesicle release.	They undergo rapid, calcium dependent exocytosis at the active zone of presynaptic terminals. Their release is tightly coupled to action potentials.

Fusion Machinery	Require high levels of calcium influx often mediated by L-type voltage gated calcium channels. Their exocytosis is regulated by proteins like Synaptotagmin IV, Munc 18 and Calcium Activated Protein for Secretion (CAPS).	Highly sensitive to low calcium levels, mainly relying on P/Q type and N type Voltage Gated Calcium Channels. They mainly use Synaptotagmin I/II, SNARE proteins, viz., Syntaxin, SNAP-25, VAMP2 and Synapsin for fast vesicle priming and fusion.
Recycling	Once fused, their membrane components are retrieved by endocytosis but often require new vesicles to be synthesized from the Golgi.	They are rapidly recycled through endocytic pathways including kiss-and-run fusion, clathrin-mediated endocytosis and bulk endocytosis.
Localisation	Found in neurons and neuroendocrine cells.	Localised exclusively at presynaptic terminals.
Physiological Role	Modulate synaptic activity, regulate neurodevelopment, control hormonal release and are involved in long lasting neuronal changes such as memory formation and stress responses.	They mediate synaptic transmission, allowing rapid communication between neurons, essential for motor control, cognition, reflexes and sensory processing.
Diseases	Dysfunctions in DCVs are linked to several neurodegenerative diseases, viz., Parkinson's, Alzheimer's, Mood disorders (Depression, Schizophrenia) and endocrine disorders like diabetes due to improper peptide hormone secretion.	Synaptic Vesicle defects contribute to neurodevelopmental disorders like Autism, ADHD, Neurodegenerative diseases like Huntington's, ALS and epilepsy due to impaired synaptic transmission.

Once the proteins reach the TGN, they are packaged into secretory vesicles for transport into the extracellular space[69]. Studies indicate that the generation of phosphatidic acid (PA) is essential for vesicle formation and budding[70,71] Additionally, small GTPases like ARF1 can activate Golgi-localised phospholipase C to facilitate

vesicle budding from the TGN[72,73] . These vesicles then transport proteins out of the cell either through constitutive or regulated secretion. In constitutive secretion, vesicles fuse with the plasma membrane without requiring an external stimulus[74]. However, regulated secretion governs the packaging of cargo into vesicles and their fusion with the plasma membrane[64,75]. Key protein families involved in this process include Rab proteins, SNAREs and dynamin. Rab proteins, small Ras-like GTPases located on vesicle surfaces, cycle between an inactive GDP-bound state and an active GTP-bound state, which drives vesicle fusion with the plasma membrane[75]. The inactive Rab protein is masked by GDP dissociation inhibitors (GDIs) and must be reactivated upon reaching the correct compartment. This reactivation occurs when a Rab guanine nucleotide exchange factor (GEF) replaces GDP with GTP, enabling the Rab to drive vesicle budding[75]. Following the budding, SNARE protein mediate vesicle fusion and release. There are two types of SNARE proteins, viz., v-SNAREs are located on the vesicle membrane and t-SNAREs which are found on the plasma membrane. These SNARE proteins interact and form the coiled coil complex that brings the vesicle close to the plasma membrane, enabling their fusion and the release of the vesicle's contents[76].

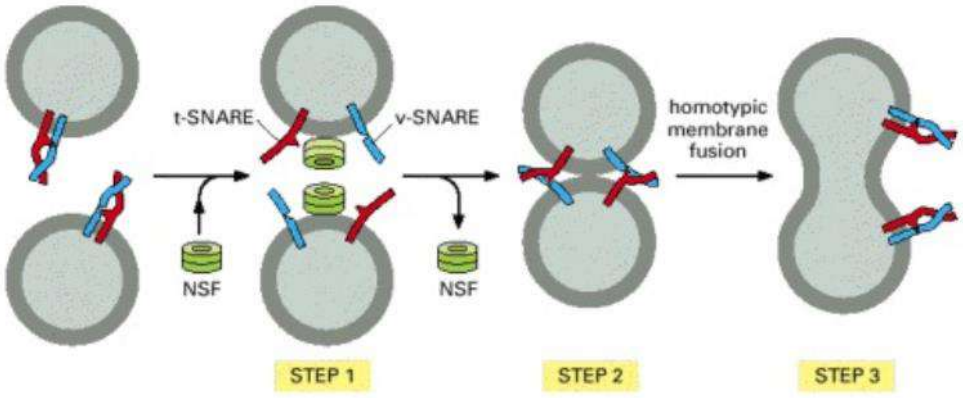

Figure 2.3: Homotypic Membrane Fusion

Source: Alberts B, Johnson A, Lewis J, Raff M, Roberts K, Walter P. Transport from the ER through the Golgi Apparatus. Mol Bio Cell 4th Ed [Internet]. 2002.

2.3 Dense Core Vesicles

Dense core vesicles (DCVs), also referred to as large dense-core vesicles (LDCVs), are specialized secretory organelles found primarily in neuronal and neuroendocrine cells[17,64]. In contrast to small synaptic vesicles (SVs) that mediate rapid neurotransmitter release at synaptic junctions, DCVs store and release neuropeptides, monoamines, and growth factors in a regulated fashion[64,77]. These vesicles play pivotal roles in long-distance intercellular communication and modulate a variety of physiological processes including neuronal development, synaptic plasticity, and hormone secretion[78,79]. The biogenesis of DCVs is initiated at the TGN, where specific cargo proteins destined for the regulated secretory pathway are selectively sorted and packaged into immature secretory vesicles[80,81]. This process involves the aggregation of soluble cargo proteins, such as prohormones and neuropeptides, in the acidic and calcium-rich environment of the TGN[18,19]. Granin family members including chromogranin A (CgA), chromogranin B (CgB), and secretogranin II (ScgII) facilitate this aggregation and contribute to cargo condensation, thereby serving as key organizers of DCV contents[3,18,19]. Following budding from the TGN, immature DCVs undergo a series of maturation steps[80]. These include acidification of the vesicle lumen via Vacuolar-type H^+-ATPases (V-ATPases), proteolytic processing of prohormones, and removal of non-DCV cargo through clathrin-mediated vesicle budding[80-82]. Such remodelling renders the vesicles competent for regulated exocytosis[82]. A variety of molecular players contribute to the formation, trafficking, and exocytosis of DCVs[19]. Granins are among the most well-characterized DCV cargo proteins[18]. Beyond facilitating protein aggregation, they also serve as precursors to biologically active peptides with hormonal and neuroactive functions [18,19]. The fusion of DCVs with the plasma membrane is mediated by the SNARE (Soluble NSF Attachment Protein Receptor) complex, which includes syntaxin-1, SNAP-25, and synaptobrevin/VAMP2[83]. This core complex, together with regulatory proteins such as Munc18 and complexin, governs the timing and probability of DCV fusion events[83,84]. Notably, the SNARE machinery in DCVs differs subtly from that in synaptic vesicles, contributing to the slower and more sustained release characteristic of dense core vesicle-mediated secretion[84]. Small GTPases, particularly Rab proteins such as Rab3, Rab27A, and Rab11, also play critical roles in the trafficking, tethering, and docking of DCVs[85,86]. Rab27A, for

instance, interacts with effectors like Synaptotagmin-like protein 1 (Slp1) and granuphilin to modulate vesicle docking and priming at the membrane[85,86]. Once formed and matured, DCVs are transported from the perinuclear region to distal cellular sites along microtubules via kinesin and dynein motor proteins[79,87]. Near the plasma membrane, actin filaments and their associated proteins help retain and localize DCVs for regulated exocytosis[79]. Triggered typically by calcium influx through voltage-gated calcium channels, DCV fusion leads to the extracellular release of their contents in a temporally controlled manner[64,87]. This process supports prolonged and diffuse signalling, in contrast to the rapid and spatially restricted release by synaptic vesicles[79]. Functionally, DCVs are indispensable for a range of physiological processes[78,82]. In endocrine cells, they mediate the release of peptide hormones such as insulin, adrenocorticotropic hormone (ACTH), and growth hormone, which are essential for metabolic regulation and stress responses[82]. In neurons, DCVs release neuropeptides like oxytocin, vasopressin, neuropeptide Y (NPY), and substance P[78]. These molecules act on both pre- and postsynaptic targets to modulate neuronal excitability, synaptic plasticity, and behaviour[78,79]. Additionally, DCVs play a significant role in neuronal development and differentiation by contributing to axon guidance, synapse formation, and neuron-glia communication[88,89]. Alterations in DCV biogenesis and secretion are implicated in several pathological conditions[15]. In type 2 diabetes, defective insulin granule formation in pancreatic β-cells has been observed[90]. In neurodegenerative disorders such as Alzheimer's and Parkinson's disease, misregulation of neuropeptide secretion may contribute to disease progression[15]. Furthermore, genetic mutations affecting proteins involved in DCV trafficking and exocytosis, such as Rab27 or granins, have been associated with neurodevelopmental disorders, including autism and epilepsy[15]. Recent advances in imaging and molecular biology have provided deeper insights into DCV dynamics[91,92]. Techniques such as live-cell imaging with NPY-pHlourin, single-vesicle tracking, and the use of the Retention Using Selective Hooks (RUSH) system have enabled high-resolution analysis of DCV trafficking and release[91,92]. In conclusion, DCVs are integral components of the regulated secretory pathway and serve vital roles in neuronal and endocrine communication. Their biogenesis, trafficking, and secretion are governed by a complex interplay of molecular machinery[19,64]. Dissecting these mechanisms further holds promise not only for advancing our understanding of cell

biology but also for identifying therapeutic targets in disorders of secretion and signalling[64].

2.4 The Granin Family of Proteins

Granins are a class of acidic, heat-stable, and hydrophilic proteins predominantly found in the secretory granules of neurons and endocrine cells[3]. They are major components of dense-core granules and play pivotal roles in the regulated secretory pathway, facilitating the sorting, storage, and release of neuropeptides and hormones[93]. First identified in chromaffin cells of the adrenal medulla[94], granins are structurally categorized into Chromogranins (Cg) and Secretogranins (Scg), with Chromogranins containing a disulfide loop near the N-terminal, a feature absent in secretogranins[19,95]. The chromogranin group includes chromogranin A (CgA) and chromogranin B (CgB), while the Secretogranin group consists of Secretogranins II to VII (ScgII-ScgVII), including ScgIII (1B1075), ScgIV (HISL-19), ScgV (7B2), ScgVI (NESP55), and proSAAS[96,97]. Chromogranins are evolutionarily conserved across vertebrates, suggesting essential biological functions[98,99], and a specific segment of the CgA sequence is known to regulate granule biogenesis and hormone storage, particularly in endocrine models such as PC12 cells[15]. In contrast, Secretogranin II is less conserved, though its core peptide secretoneurin is well retained across species[95]. Granins are proteolytically processed by protein convertases such as PC1/3 and PC2 to generate bioactive peptides, including vasostatin, pancreastatin, CgB1-41, and secretoneurin, which modulate cardiovascular, metabolic, and neuronal functions[18,100]. These proteins are synthesized in the rough endoplasmic reticulum (RER) and transported through the Golgi to the trans-Golgi network (TGN), where, they aggregate and promote dense-core vesicle formation[101] under acidic and calcium-rich conditions. CgA and CgB are involved in cargo condensation, whereas ScgIII functions as a scaffold with CgA and cholesterol to mediate granule assembly[15]. ScgV (7B2) acts uniquely as a chaperone for PC2, assisting in its maturation[19]. Beyond structural roles, granins give rise to numerous peptides with autocrine, paracrine, and endocrine functions. CgA-derived peptides like catestatin, vasostatin, and pancreastatin influence catecholamine release, cardiovascular dynamics, and insulin signaling[102]. Secretoneurin from ScgII supports neurogenesis and neuronal migration[100,103], while CgB participates in vesicle docking through

interactions with SNAP-25 and syntaxin[104]. Secretogranin VII (VGF), though structurally divergent, is categorized among granins due to its expression and processing profile[95]. VGF is an NGF-inducible gene expressed in neurons and neuroendocrine cells, producing peptides such as TLQP-21 and NERP-1/2, which regulate synaptic plasticity, energy balance, neurogenesis, and mood[105,106]. Granin expression in the brain is region-specific; for instance, CgB and ScgII are enriched in the cortex and hippocampus and co-localize with synaptic proteins like VAMP2, suggesting roles in neurotransmission[100,103]. VGF peptides are also highly expressed in the hippocampus and hypothalamus, where they modulate stress responses, learning, and memory[107]. Clinically, granins are valuable biomarkers; CgA levels serve as diagnostic and prognostic indicators for neuroendocrine tumours, including pheochromocytomas and carcinoids[108]. Alterations in Granin expression are associated with neurodegenerative disorders such as Alzheimer's disease, where CgB levels and peptide processing are dysregulated[109]. Moreover, VGF expression is diminished in Alzheimer's and major depressive disorder, with its peptides proposed as early cerebrospinal fluid biomarkers[110]. In summary, granins serve multifaceted roles from dense-core granule formation to neuropeptide generation and function. While structural aspects are relatively well-characterized, emerging research on Granin-derived peptides, especially from VGF, reveals nuanced regulatory roles in health and disease, making it necessary to conduct further mechanistic studies for therapeutic exploration.

2.5 Bioactive Peptides Derived from the Granin Family

The various bioactive peptides derived from the Granin Family, its functions and location in various cell types are listed in the table below: [2,100,105,106,111]

Figure 2.4

Granin Precursor	Bioactive Peptides	Known Functions	Tissue/Cell Types
Chromogranin A (CgA)	Catestatin (CgA352-372)	Inhibits catecholamine release, antimicrobial, modulates BP	Adrenal medulla, sympathetic neurons
	Vasostatin I (CgA1-76), II	Antiadrenergic, vasodilatory role	Endothelium, cardiac tissue
	Pancreastatin (CgA250-301)	Inhibits insulin/glucagon secretion, modulates metabolism	Pancreatic islets, neuroendocrine cells
	Serpinin	Enhances granule biogenesis, neuroprotective agent	Pituitary, CNS neurons
Chromogranin B (CgB)	Secretolytin (CgB614-626)	Stimulates exocytosis, antimicrobial activities	Neuroendocrine cells
	PE-11 (CgB chromofungin)	Vasoactive, antimicrobial activities	Brain, adrenal medulla
Secretogranin II (ScgII)	Secretoneurin (SgII154-186)	Neurotrophic, chemotactic, and angiogenic function	CNS, endocrine tissues
Secretogranin III (ScgIII)	(No well-defined peptide)	Granin chaperone for CgA and hormone sorting at TGN	Pituitary, adrenal gland
Secretogranin IV (ScgIV)	(Poorly characterised)	Putative Granin, function unclear	Adrenal, neuroendocrine
Secretogranin V (7B2)	7B2 peptide	Chaperone for prohormone convertase 2 (PC2)	Brain, endocrine pancreas
Secretogranin VI (NESP55)	NESP55-derived peptides	Modulates stress and behaviour	Brain, adrenal medulla
Secretogranin VII (VGF)	TLQP-21 (VGF556-576)	Enhances energy expenditure, neuroprotective, and anti-nociceptive	Hypothalamus, adipose, CNS
	NERP-1 (VGF529-546), NERP-2	Regulates vasopressin release, water homeostasis	Hypothalamus

Granin Precursor	Bioactive Peptides	Known Functions	Tissue/Cell Types
	AQEE-30	Synaptic plasticity, antidepressant	Hippocampus, cortex
	HFHH-34	Anti-depressive, neuroprotective agent	Hippocampus
	LQEQ-19	Enhances LTP, neurotrophic agent	Brain

2.6 Secretogranin VII and Regulated Exocytosis

Neurotrophins such as nerve growth factor (NGF), brain-derived neurotrophic factor (BDNF), and neurotrophin-3 (NT-3) have been extensively studied for their vital roles in the development, survival, and synaptic plasticity of neurons in both the peripheral and central nervous systems[112,113]. They exert their effects primarily through binding to tropomyosin receptor kinases (TrkA/B/C), initiating complex intracellular signalling cascades that regulate gene transcription and protein translation necessary for neuronal function[114]. In contrast to the wealth of knowledge on neurotrophin action in classical neuronal circuits, relatively less is understood about their roles in neuroendocrine systems, particularly within the hypothalamus and pituitary gland, which are key regulators of metabolism, reproductive function, stress response, and feeding behavior[115,116]. This gap in knowledge is significant, as the hypothalamic-pituitary axis integrates both neuronal and endocrine signals to maintain physiological homeostasis. One fruitful strategy for deciphering neurotrophin signalling pathways has been the identification and analysis of immediate-early genes or downstream effectors that are transcriptionally regulated by neurotrophin stimulation. These neurotrophin-responsive genes often encode proteins involved in axon outgrowth, vesicle trafficking, and synaptic modification, thereby serving as functional mediators of neurotrophic activity[117]. Secretogranin VII, also known as VGF (non-acronymic), is a neuropeptide precursor that belongs to the chromogranin/secretogranin family of acidic secretory proteins[95]. It was initially identified as a nerve growth factor (NGF)-responsive gene in PC12 cells, highlighting its role in neuronal differentiation[113]. The human VGF gene is located on chromosome 7q22 and encodes a 617-amino acid precursor protein[1]. Notably, VGF is not an acronym but was designated based on its identification during studies on NGF-induced gene expression[1]. The VGF precursor undergoes extensive proteolytic processing by prohormone convertases such as

PC1/3 and PC2 at paired basic residues, generating a diverse range of bioactive peptides with distinct physiological functions[18,96]. Among the most studied peptides derived from VGF are TLQP-21, TLQP-62, NERP-1, NERP-2, AQEE-30, and HHPD-41[1,118].

2.7 VGF-Derived Peptides: Expression and Function in the Neuroendocrine and Central Nervous Systems

VGF and its derived peptides are widely expressed in the central and peripheral nervous systems, with particularly high expression levels in hypothalamus, pituitary gland, adrenal medulla, and various brain regions including the hippocampus, cortex, striatum, and amygdala[20,119]. In peripheral tissues, VGF is also expressed in pancreatic islets, adipose tissue, and the gastrointestinal tract, suggesting systemic roles beyond the nervous system[119]. In the neuroendocrine context, VGF-derived peptides such as NERP-1 and NERP-2 (Neuroendocrine Regulatory Peptides) have been shown to modulate vasopressin release, thus contributing to the regulation of fluid homeostasis and osmoregulation[118]. These peptides are predominantly produced in the hypothalamus and pituitary and act on magnocellular neurons to control water balance in response to osmotic stress[20]. Furthermore, VGF expression is regulated by stress and circadian signals, and its peptides are implicated in the modulation of the hypothalamic-pituitary-adrenal (HPA) axis, including corticosterone secretion, which is central to stress adaptation[20,105]. This positions VGF as a key neuroendocrine integrator of external and internal physiological cues. Several VGF-derived peptides, particularly TLQP-21, are known to influence energy balance, lipolysis, and thermogenesis, primarily by acting on hypothalamic neurons and peripheral adipocytes[2,120]. TLQP-21 binds to the complement 3a receptor 1 (C3aR1), triggering intracellular calcium signalling and enhancing energy expenditure, suggesting therapeutic potential in obesity and metabolic disorders[2]. In the central nervous system, VGF-derived peptides also play pivotal roles in synaptic plasticity, long-term potentiation (LTP), and memory consolidation. For instance, AQEE-30 and LQEQ-19 peptides, expressed in the hippocampus, are upregulated following learning and are believed to act as neuromodulators to enhance synaptic strength and plasticity[21,106]. Moreover, VGF mRNA levels are modulated by neuronal activity and antidepressant treatment, pointing to a role in mood regulation[105]. Experimental

studies have demonstrated that VGF knockout mice exhibit increased anxiety- and depression-like behaviours, impaired synaptic function, and altered metabolic profiles, further validating the multifunctional role of VGF in behavioural homeostasis and neuronal resilience[119,121].

2.8 Role of VGF in various Neuroendocrine systems

Functionally, VGF and its derived peptides play crucial roles in the neuroendocrine system, metabolism, synaptic plasticity, mood regulation, and neuroprotection[115]. VGF is highly expressed in the hypothalamus, pituitary, adrenal medulla, and several regions of the central nervous system (CNS), including the cortex, hippocampus, and amygdala[20]. In the neuroendocrine context, VGF peptides modulate the secretion of hormones such as vasopressin and corticosterone, thus influencing fluid balance and stress responses[20]. One of the best-characterized peptides, TLQP-21, enhances sympathetic nervous system activity, increases energy expenditure, and reduces adiposity, implicating it in the regulation of energy balance[2]. This aligns with findings from VGF knockout mice, which exhibit hyperactivity, leanness, and impaired thermoregulation, underscoring VGF's role in metabolic homeostasis[119]. Beyond metabolism, VGF has significant functions in synaptic activity and plasticity[106]. As an activity-regulated gene, VGF expression is upregulated in response to neuronal activity and brain-derived neurotrophic factor (BDNF)[105]. In the hippocampus, VGF peptides contribute to the enhancement of long-term potentiation (LTP) and synaptic strength[106]. VGF-deficient mice display impairments in learning and memory, indicating a role in cognitive function[119]. Peptides like AQEE-30 and TLQP-62 promote neurite outgrowth and synapse formation, further suggesting their involvement in neural development and connectivity[121]. Moreover, VGF has emerged as a key modulator of mood and emotional behavior[122]. Its expression is reduced in models of depression and chronic stress, while treatment with antidepressants or physical exercise increases its levels[105,115]. TLQP-62, in particular, has demonstrated antidepressant-like effects in preclinical behavioural assays[122]. Physiologically, VGF serves multiple roles both in the CNS and peripheral systems[18]. In the CNS, it regulates circadian rhythms, synaptic transmission, and memory consolidation[115]. Peripherally, VGF is found in pancreatic islets, adipose tissue, and the gastrointestinal tract, where it influences

insulin secretion, lipid metabolism, and gut motility[18,123]. Such diverse localization explains its widespread physiological implications[118]. In disease contexts, altered VGF expression has been implicated in a range of neurological, psychiatric, and metabolic disorders[124,125]. In Alzheimer's disease (AD), VGF levels are significantly reduced in cerebrospinal fluid (CSF) and postmortem brain tissue, making it a promising biomarker for early diagnosis and progression[115,124]. Similarly, in amyotrophic lateral sclerosis (ALS), decreased levels of VGF have been observed in the spinal cord and CSF of both patients and animal models, suggesting a role in motor neuron survival[125]. Parkinson's disease (PD) has also been linked to dysregulated expression of VGF peptides, although the specific mechanisms remain less well understood[126]. In psychiatric disorders, such as depression, anxiety, schizophrenia, and bipolar disorder, alterations in VGF expression and processing have been reported[127]. VGF expression is particularly sensitive to stress and neurotrophic signalling, and the administration of its peptides exerts anxiolytic and antidepressant-like effects in rodents[105,122]. Moreover, given its impact on insulin release and glucose metabolism, VGF is also associated with metabolic disorders like obesity and type 2 diabetes[126]. TLQP-21 enhances insulin secretion and improves glucose tolerance, making VGF-derived peptides attractive candidates for metabolic disease intervention[2]. Given its diverse roles and disease associations, VGF is increasingly recognized as both a potential biomarker and a therapeutic target[115]. Ongoing clinical studies are investigating VGF peptide levels in CSF and plasma for neurodegenerative disease diagnostics[124]. Simultaneously, peptide derivatives like TLQP-21 and TLQP-62 are being explored for their therapeutic potential in neurodegenerative, mood, and metabolic disorders[18,118]. However, further research is required to fully elucidate the regulation of VGF proteolysis, receptor interactions, and downstream signalling mechanisms[96,127]. In summary, VGF stands out as a multifunctional protein with profound implications in neurobiology, endocrinology, and disease, warranting deeper investigation into its biological pathways and translational applications[115].

Chapter 3
Materials and Methods

Chapter 3

Materials and Methods

3.1 Cell Culture

Rat PC12 cells, originally established by Greene and Tischler in 1976[6], were kindly provided by Dr. Nitish Mahapatra from Indian Institute of Technology Madras. All experiments were conducted using early passage cells which were routinely treated with mycoplasma removal reagent (MP Biomedicals, 30-50044). Cells were cultured using Dulbecco's Modified Eagle Medium (DMEM) GlutaMAX (Gibco, 12100046), supplemented with 10% horse serum (Gibco, 16050114), 5% heat-inactivated fetal bovine serum (FBS; Sigma-Aldrich, F7524), 25 mM HEPES (Sigma-Aldrich, H3784), and 1% antibiotic-antimycotic solution (Gibco, 15240062). Cultures were maintained at 37°C in a humidified incubator with 6% CO_2 atmosphere[128].

3.2 Generation of VGF knockout cells by CRISPR-Cas9 method

Knockouts of VGF were generated using CRISPR-Cas9 genome editing. Two guide RNAs (gRNA) were designed targeting exon 3 using the CHOP-CHOP tool and cloned in the px459 v2.0 vector.

The guide RNA sequences and validation primer sequences are as follows:

VGF KO1 gRNA FP: 5'-**CACCG**CACGTTGCCAGCATCCGTC-3'

VGF KO1 gRNA RP: 5'-**AAAC**GGACGGATGCTGGCAACGTG-3'

VGF KO2 gRNA FP: 5'-**CACCG**GGCGTACCAAAGTCTAAGT-3'

VGF KO2 gRNA RP: 5'-**AAAC**ACTTAGACTTTGGTACGCC-3'

VGF KO1 val FP: 5'-CACGTTGCCAGCATCCGTC-3'

VGF KO1 val RP: 5'-TCTCCCTGGTCCTGAGGCT-3'

VGF KO2 val FP: 5'-CCGAGTCAATCTGGAGAGC-3'

VGF KO2 val RP: 5'-TTGCTGCGTCTCCTGCAG-3'

The cloned plasmids were validated by Sanger sequencing from ATPC, Regional Centre for Biotechnology. 4 x 10^6 cells were seeded in a 6-well plate previously coated with 1X Poly-L-lysine (Sigma-Aldrich, CAS: 25988-63-0) and transfected with the sequenced plasmids after 12 hours of seeding. After 48 hours of transfection, the cells were subjected to puromycin selection (2.5 µg/ml puromycin in PC12 Complete media) for 6 days. The cells were shifted to a 100 mm dish previously coated with 0.2% Gelatin (Fluka, 48723) and the selected population of single cell clone was picked using cloning cylinder and then shifted to a 48-well plate with maintenance media (PC12 complete media with 0.25 µg/ml puromycin). Approximately 8-10 colonies per guide were picked, grown and validated for VGF knockout using western blotting, and immunofluorescence.

3.3 Transfections

All the transfections were performed using Metafectene (Biointex, T020-5.0) as per the manufacturer's protocol[129]. Cells were seeded 4 hours prior to transfection. Complete media was replaced with serum-free media for 30 minutes to induce serum starvation in the cells. Plasmid DNA solution and Metafectene solution (1:1.25) were prepared separately in serum-free media. Both solutions were then mixed and incubated for 20 minutes at room temperature to allow complex formation. Post incubation, DNA-metafectene complex was gently added dropwise to the cells in DMEM media with serum and incubated for 12 hours in a humidified incubator with 6% CO2 at 37°C. After the incubation period, the transfection media was replaced by fresh complete media. All experiments were performed 48 hours post-transfection.

3.4 Mammalian Expression Constructs

Name	Make	Catalog No.
NPY-pHlourin	A kind gift from Sebastian Barg, Uppsala	N/A
NPY-pHTomato	Addgene	83501
VGF-GFP	A kind gift from Stephen R. Salton's Lab, New York	N/A
Synaptophysin-pHlourin	Addgene	168510

3.5 Immunoblotting

WT and KO cells were lysed using RIPA buffer (10 mM Tris-HCl (Sisco Research Laboratory Pvt. Limited, 37969/ 77-86-1), 150 mM NaCl (MP Biomedicals, 194848), 1 mM NaVO4 (Sigma Aldrich, S-6508), 30 mM Na4P2O7 (Sigma Aldrich, 011K0307), 50 mM NaF (Sigma Aldrich, 7681-49-4), 1% Nonidet P-40 (Sigma Aldrich), 0.1% SDS (Affymetrix USB Products, 151-21-3), 1 mM PMSF (Sigma Aldrich, 52K0052), 1% Triton X-100 (Sigma Aldrich), 0.5% C24H39NaO4 (Sigma Aldrich, 145224-92-6), and dissolved protease inhibitor cocktail (Roche Diagnostics, 11714900) in water, pH 7.4). The protein contents of the cell lysate were quantified using a BCA Protein Assay Kit (TAKARA) following the manufacturer's protocol[130]. The samples were separated using a 10% or 12% SDS-polyacrylamide gel and transferred onto nitrocellulose membranes. After blocking with 5% Skimmed milk (Himedia, 310-127-6) for two hours at room temperature, membranes were incubated with primary antibodies overnight at 4℃ or for 1 hr at room temperature 37℃, followed by incubation with secondary antibodies for 2 hours at room temperature (Peroxidase AffiniPure Goat Anti-Rabbit IgG (H+L) Jackson Immuno Research 111-035-003, Peroxidase AffiniPure Goat Anti-Mouse IgG (H+L) Jackson Immuno Research 115-035-003). The membrane was washed thrice with 1x TBS-T for 10 minutes after primary and secondary antibody incubation

to remove excess antibodies. ECL was prepared using the previously described protocol[131], and bands were visualized using the Uvitec Mini HD9 gel imaging system. Densitometry quantifications were done using ImageLab (6.0.1)[132].

3.6 Immunocytochemistry

For immunocytochemistry, a previously standardised protocol was followed[133]. Cells were seeded onto 0.2% Gelatin (Fluka, 48723) coated 12mm coverslips. Cells were then washed gently with 1X PBS (Gibco, 21600-069), and fixed in 4% paraformaldehyde for 20 mins at 37°C followed by three gentle washes of 5 minutes each with 1X PBS . To permeabilize the cells, cells were incubated with 0.2% Triton X-100 (Sigma Aldrich, 9002-93-1) for 20 minutes. The permeabilized cells were again washed twice for 5 minutes each with 1X PBS and blocked with 1% bovine serum albumin (BSA) (Sigma, A4503) for 1 hour to avoid any non-specific binding. The cells were then incubated overnight with primary antibodies at 4°C. To remove excess antibodies, the cells were washed three times with 1X PBS for 5 minutes each and then incubated with fluorophore-conjugated secondary antibodies (Invitrogen Rabbit Alexa Fluor™ 647(A-31573), Mouse Alexa Fluor™ 647(A-31571), Rabbit Alexa Fluor™ 594(A-11012), Mouse Alexa Fluor™ 594(A-11005), DAPI (Sigma Aldrich, F6057)). After the secondary antibody incubation, the cells were washed thrice with 1X PBS for 5 minutes each and mounted on glass slides using Flouroshield™ with DAPI (Sigma Aldrich, F6057). Immunofluorescent images were captured using a Nikon A1HD25 confocal microscope under a 60X oil objective (NA 1.4) with appropriate filter settings at 2048*2048-pixel resolution.

3.7 Stimulated Emission Depletion (STED) Microscopy

WT and KO cells were seeded onto 1X PLL (Sigma-Aldrich, 25988-63-0) coated 15mm coverslips with 1 x 10^5 cells per coverslip. The next day, cells were fixed with 4% PFA for 15 minutes to preserve cellular architecture while maintaining antigenicity. The fixative was subsequently removed, and the cells were washed three times with 1X PBS for 5 minutes each to eliminate residual PFA and reduce background fluorescence. The subsequent immunostaining was based on established immunocytochemistry protocols with modifications optimized for STED imaging. Cells were blocked in 2% BSA prepared in 1X PBS for 1 hour at room

temperature to prevent non-specific antibody binding. Secretogranin II (20357-1-AP) was given as the primary antibody and incubated overnight at 4°C. The following day, coverslips were washed with 1X PBS thrice and secondary antibody incubation was performed using Alexa Fluor™ 594-conjugated goat anti-rabbit IgG (Thermo Fisher Scientific, A-11012), diluted 1:500 in the same blocking buffer. This fluorophore is compatible with STED imaging due to its optimal photostability and efficient depletion at 775 nm[134]. After immunolabeling, cells were mounted using ProLong™ Glass Antifade Mountant (Thermo Fisher Scientific) without DAPI to avoid spectral overlap in the far-red emission range used for STED. Coverslips were allowed to cure for at least 24 hours in the dark at room temperature before imaging. Super-resolution imaging was performed using the Leica Stellaris 8 STED microscope equipped with a 100X oil immersion objective lens (numerical aperture 1.4), offering high photon collection efficiency and spatial resolution. Alexa Fluor™ 594 was excited using the appropriate laser line, and a 775 nm pulsed depletion laser was applied for STED imaging to achieve sub-diffraction spatial resolution, in line with previously reported imaging conditions[135,136].

3.8 Stimulus Coupled Secretion Assay

A stimulus-coupled secretion assay was performed in PC12 cells according to a previous protocol[137,138]. WT PC12 and VGF KO cells were seeded at high density (~80% confluency) on 60 mm tissue culture dishes (Tarsons) to ensure optimal secretory granule maturation and synaptic-like vesicle formation, which are known to depend on cell density and differentiation state in PC12 cells[81]. 24 hours post cell seeding, cells were incubated with basal buffer (150 mM NaCl, 5 mM KCl, 2 mM $CaCl_2$, 10 mM HEPES; pH 7.4) and stimulation buffer (150 mM NaCl, 100 mM KCl, 2 mM $CaCl_2$, 10 mM HEPES; pH 7.4) for 20 minutes at 37°C in a humidified cell culture chamber with 5% CO_2. Both buffers were pre-warmed to maintain physiological conditions during incubation. The supernatant was then collected, whereas cell lysates were prepared and quantified using Bicinchoninic Acid Assay kit (Takara) for Immunoblotting. Supernatants and cell lysates were collected and run in SDS - PAGE and probed with CgB (Proteintech, 14968-1-AP,1:5000), B-Tub (Proteintech,10094-1-AP,1:20000) for all the lines.

3.9 Live cell imaging

WT and KO cells were seeded onto Poly-L-lysine-coated (Sigma Aldrich, P2636) 15 mm coverslips in 6-well plates with a density of 2 × 10^6 cells/well, and were then transiently transfected with NPY pH Tomato (Addgene) and NPY-pHlourin to assess regulated secretion and synaptophysin-pHlourin (Addgene) to assess secretion of synaptic-like vesicles. On the day of the experiment, cells were rinsed with basal buffer (150 mM NaCl, 5 mM KCl, 2 mM CaCl2, 10 mM HEPES; pH 7.4), and coverslips were placed in an open imaging chamber (Life Cell Instruments, Korea). The images were captured using Nikon Eclipse Ti2 at 100X oil (1.30) at 300 ms in the Tyrode's buffer (basal), after which stimulation was given at 300 ms for 15 sec in the Tyrode's buffer (stimulation) containing 100mM KCl. After the end of the experiment, 100 mM NH4Cl-containing Tyrode's buffer was added to capture the total fluorescence of the cells. Captured time-lapse movies were analysed using ImageJ software, and after background subtraction, the change in puncta intensity per cell (Δf) after 100 mM KCl stimulation, compared to basal fluorescence (f0), was plotted as Δf/f0.

3.10 Constitutive secretion

Secretion fractions from unstimulated cells were assessed for the constitutive release of proteins in basal conditions using Coomassie staining by SimplyBlueTM SafeStain (Invitrogen, LC6060)[137,139]. Cells were seeded in a density of 10^6 cells in 0.2% gelatin coated 60 mm dishes and allowed to grow for 24 hours. The following day, the media was replaced by Tyrode's buffer (basal) (150 mM NaCl, 5 mM KCl, 2 mM CaCl2, 10 mM HEPES; pH 7.4) and cells were incubated for 3 hours. The cell lysates and supernatants were then processed and resolved on a 10% SDS-polyacrylamide gel. The gel was carefully removed from the electrophoresis apparatus and washed twice with Milli-Q water followed by one hour incubation in SimplyBlueTM SafeStain (Invitrogen) at room temperature with gentle shaking. Post staining, excess stain was removed by washing the gel twice with Milli-Q water. The gel was imaged in the Azure c300 gel imaging system, and the detected bands were quantified using ImageLab (6.0.1). Further, for estimating constitutive secretion using a marker, immunoblotting was carried out and probed for HSP90

(Proteintech,13171-1-AP, 1:1000). Bands were visualized using the Uvitec Mini HD9 gel imaging system[131].

3.11 Dextran Uptake Assay

A previously published protocol was used to understand the modes of exocytosis[140]. In brief, WT and KO cells were washed once with 1X PBS and twice with extracellular bath solution (145 mM NaCl, 2.8 mM KCl, 2 mM $CaCl_2$ and 100 mM HEPES, pH 7.4) and then incubated for 5 minutes with 50uM dextran (10 and 40 kDa, Invitrogen D1817 and D1842) in 100 mM KCl containing extracellular bath solution at 37˚C. The unbound dye was washed out with the previously mentioned bath solution (without Ca2+) and immediately fixed with 4% PFA for 20 minutes followed by washing with 1X PBS twice before mounting. Confocal imaging was done, as previously mentioned, where a Z-series of 1µm optical sections were scanned. For analysis, the consecutive optical sections were projected in ImageJ, and the total numbers of dextran fluorescent puncta per cell were determined and normalized according to the area of the cell.

3.12 Endolysosomal Assay

In this assay, 2 x 10^5 cells seeded on coverslips in a 12-well plate from both WT and KD cells were subjected to incubation at 37˚C with 1% 10kDa Dextran (50um) in DMEM incomplete media (i.e., no serum and antibiotic) for 30 mins. After 30 minutes, the cells were washed twice with 1X PBS and then incubated with DMEM complete media without dextran (this is referred to as the washout step). The individual coverslips were fixed at 0 min, 30 mins, 1 hr, 2 hrs, 4 hrs and 6 hrs post-washing, respectively, with 4% PFA. Confocal imaging was done, as previously mentioned, where a Z-series of 1µm optical sections were scanned. For analysis, the consecutive optical sections were projected in ImageJ, and the total numbers of dextran fluorescent puncta per cell were determined and normalised according to the area of the cell.

Chapter 4
Results

Chapter 4

Results

4.1 Cloning of CRISPR-Cas9 Guide RNAs Targeting the Rat VGF Gene

To generate VGF knockout in PC12 cells, guide RNAs (gRNAs) targeting exon 3 of the rat VGF gene were designed using the online tool CHOPCHOP, which optimises high on-target efficacy with minimal predicted off-target effects. The selected gRNA oligonucleotides were successfully annealed and phosphorylated (Fig. 4.1A). The PX459 vector (pSpCas9(BB)-2A-Puro), used for CRISPR-mediated genome editing, was linearised by BbsI digestion. A distinct 9174 bp band corresponding to the linearised vector was observed on 0.8% agarose gel electrophoresis (Fig. 4.1B, 4.1C). The digested vector was purified using MN gel extraction kit and run again on agarose gel to confirm recovery post-elution (Fig. 4.1D). The annealed oligos were ligated into the linearised PX459 vector and transformed into *E. coli* DH10β competent cells (Fig. 4.1B). Following transformation, bacterial colonies were screened using colony PCR with U6 promoter-specific forward primer and gRNA-specific reverse primer (Fig. 4.1E). PCR screening yielded a specific 273 bp product, indicating successful insertion of the gRNA sequence (Fig. 4.1F, 4.1G). Positive clones were further validated by Sanger sequencing, confirming the correct orientation and sequence of the inserted gRNA within the PX459 backbone (Fig. 4.1H, 4.1I). These verified constructs were subsequently used for transfection into PC12 cells for generating KOs of VGF.

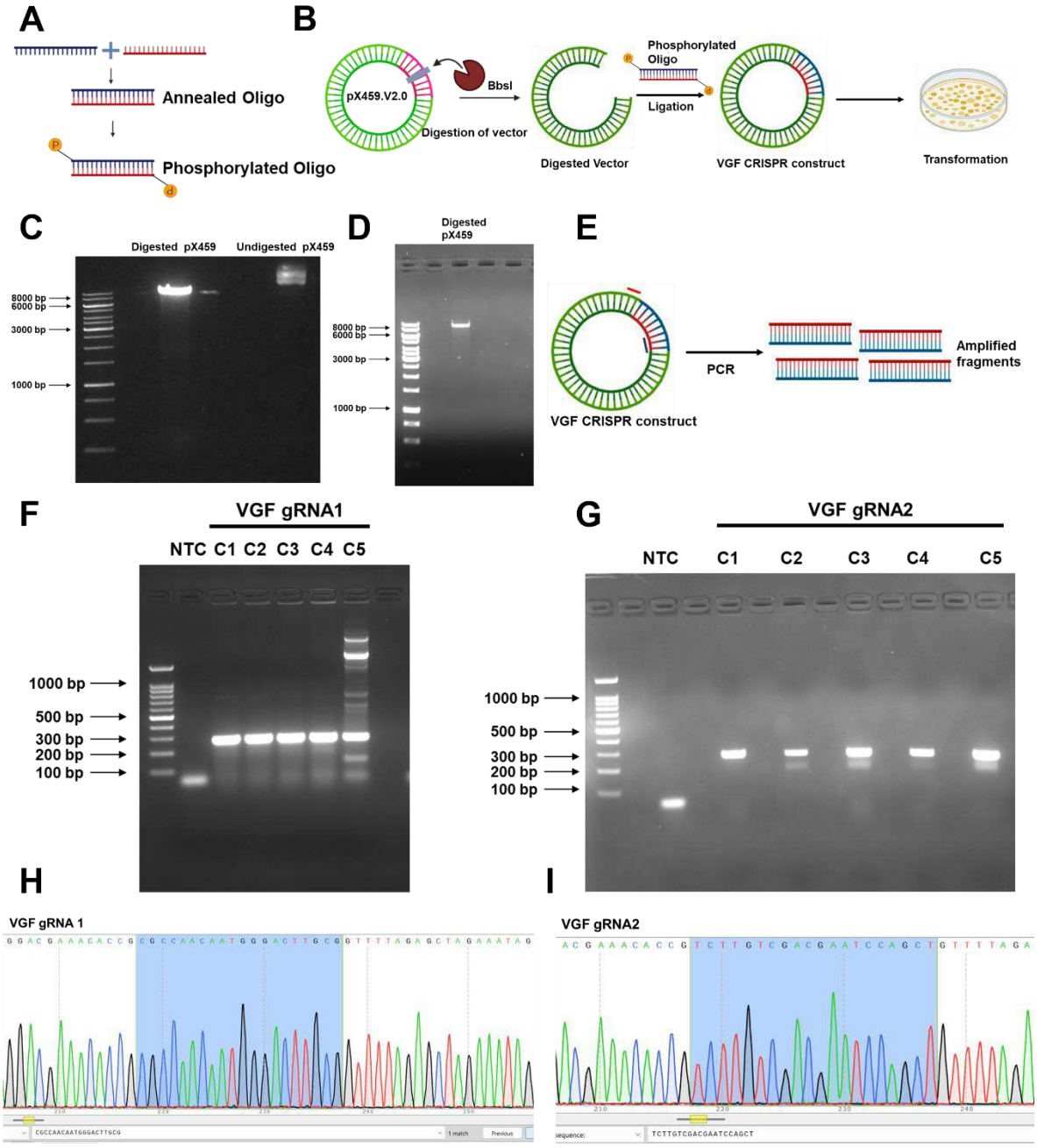

Figure 4.1: Cloning of gRNAs in the PX459 vector. A. Schematic showing annealing and phosphorylation of oligos (guide sequences). **B.** Schematic showing the cloning procedure. **C.** BbsI digested PX459 vector after running on 0.8% agarose gel. **D.** Gel extracted sample run on a 0.8% agarose gel post elution. **E.** Schematic showing PCR of the VGF CRISPR construct. **F.** PCR products of the screened colonies from gRNA1 and **G.** gRNA2 after running on 1.8% agarose gel. **H.** Sanger sequencing of gRNA1 and **I.** gRNA2 shows successful insertion of the guide RNA into the PX459 vector.

4.2 Generation and Validation of VGF Knockout PC12 Cells Using CRISPR-Cas9 method

VGF (non-acronymic), a member of the Granin family, is a neurosecretory protein enriched in neuroendocrine and neuronal cells. It plays essential roles in neuropeptide processing, energy homeostasis, synaptic plasticity, and potentially in dense-core vesicle biogenesis and trafficking; however, its precise molecular function in regulated secretion remains poorly characterized[26,141]. To elucidate the functional role of VGF in DCV trafficking and secretion, we employed a CRISPR-Cas9-mediated loss-of-function approach to generate a VGF KO model in the Rat PC12 cell line, a widely used neuroendocrine model for studying vesicle dynamics and regulated exocytosis[66,81]. Two independent guide RNAs (gRNAs) were designed to target distinct sequences within Exon 3 of the Rat VGF gene, a coding region common to all known VGF isoforms. PC12 cells were transfected with the VGF gRNA PX459 constructs using Metafectene following the manufacturer's protocol. 48 hours post-transfection, cells were subjected to puromycin selection (2.5 µg/mL) for 72 hours. Cells that grew under puromycin selection were subjected to dilution and plating at clonal density to facilitate single cell colony isolation (Fig 4.2A). Individual clones were screened for VGF expression by immunoblotting and immunocytochemistry using a rabbit anti-VGF antibody. Clones that exhibited complete loss of VGF protein expression were further validated at the genomic level. Genomic DNA was isolated from the selected clones, and the region flanking the sgRNA target sites in Exon 3 was PCR-amplified and analysed by Sanger sequencing. The sequencing data revealed the presence of insertions or deletions (indels) at the target sites, resulting in frameshift mutations. From sequencing results, it was seen that in case of guide 1, there was a deletion mutation (Fig. 4.2B) and in case of guide 2, a transversion mutation (change of Guanine to Thymine) took place (Fig. 4.2C). Immunoblot analysis confirmed the absence of VGF protein in the knockout clones compared to WT PC12 cells (Fig. 4.2D). Additionally, immunocytochemistry showed complete loss of VGF immunoreactivity in the KO lines, corroborating the successful disruption of VGF expression (Fig. 4.2E). Together, these results validate the establishment of a CRISPR-mediated VGF

knockout PC12 cell line, which can be further utilized to investigate the role of VGF in DCV maturation, trafficking, and stimulus-coupled secretion.

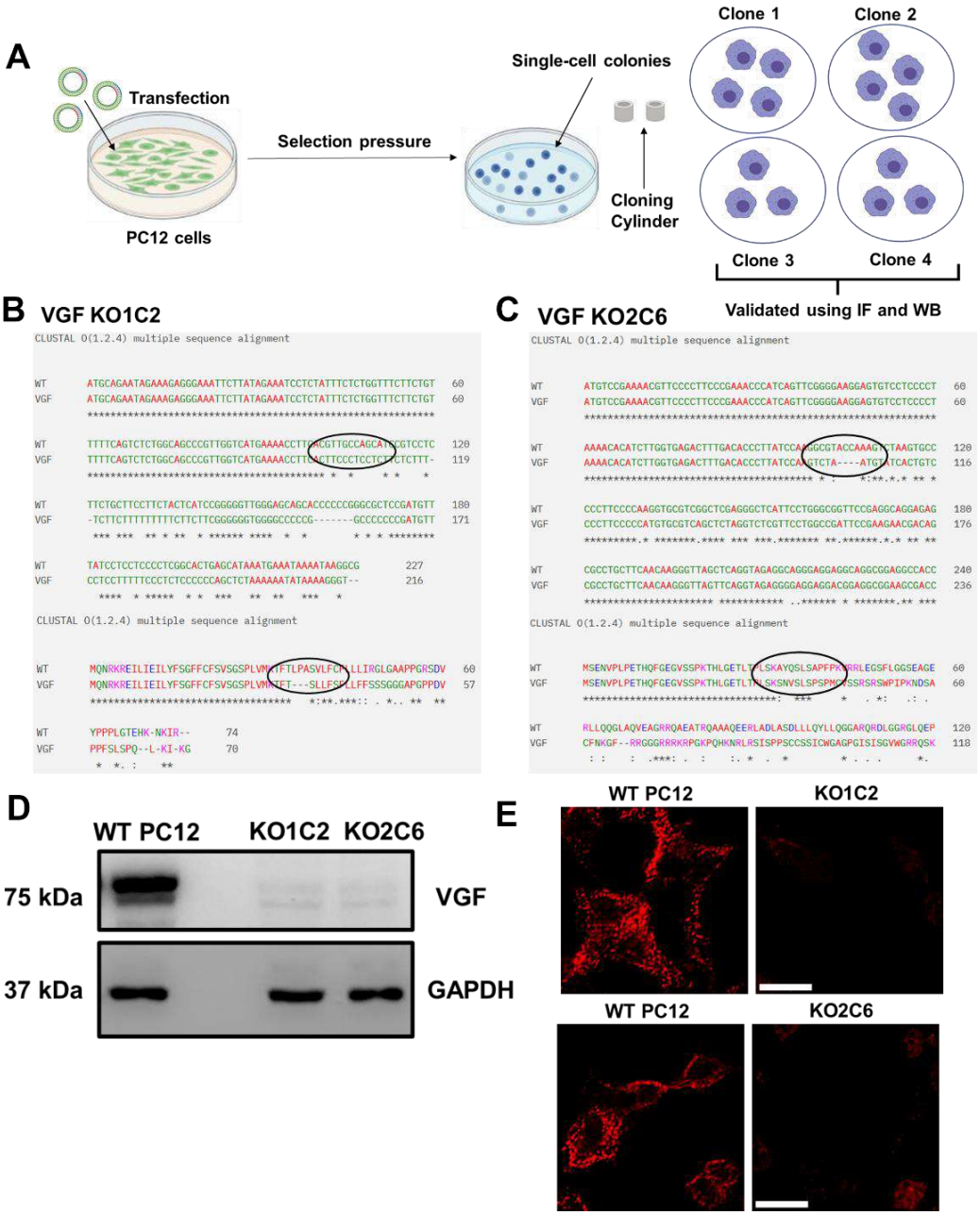

Figure 4.2: Generation and Validation of VGF KO PC12 cells. A. Schematic showing transfection of the VGF CRISPR construct followed by antibiotic selection and isolation of single-cell colonies. **B.** Sanger sequencing shows deletion of guanine base resulting in a frameshift mutation in the screened colony of guide 1. **C.** Sanger sequencing shows a transversion mutation from guanine to thymine in the screened colony of guide 2. **D.** Immunoblot showing absence of VGF protein in the sequence-validated knockout clones in both guides. **E.** Immunocytochemistry revealed loss of VGF immunofluorescence in the validated KO lines. Scale Bar 5µm.

4.3 Loss of VGF Impairs Regulated Secretion in PC12 Cells

Although the physiological relevance of VGF-derived peptides is well established in multiple biological processes, including energy homeostasis, synaptic plasticity, and neuroendocrine function, the precise molecular role of VGF in the process of regulated exocytosis remains largely unresolved[1,142]. VGF is a Granin protein that localizes to DCVs, where it is co-packaged with other Granin family members such as Chromogranins and Secretogranins. These granins are known to regulate the sorting, condensation, and maturation of secretory cargo, as well as the dynamics of vesicle fusion with the plasma membrane[3,18]. The localization of VGF to DCVs and its co-expression with granins suggest that VGF might participate directly in modulating vesicle trafficking, docking, or fusion during stimulus-induced secretion. Moreover, emerging evidence implicates DCV-resident proteins in coordinating the readily releasable pool (RRP) of vesicles during calcium-triggered exocytosis[66,143], further underscoring the need to functionally study VGF's role in this pathway. This forms the rationale for examining the status of regulated exocytosis in VGF-deficient cells. To assess the functional consequences of VGF knockout in regulated secretion, stimulus-coupled secretion assay[138] was performed. This assay is designed to evaluate the ability of cells to release vesicular contents in response to depolarization-induced calcium influx[143]. The WT and KO cells were incubated in basal and stimulation conditions using the Tyrode's buffer. Stimulation was induced using a solution containing high levels of potassium (KCl), which causes cells to depolarise leading to triggered Ca2+ influx, enabling the release of the readily releasable pool of DCV clusters[144]. The released fractions (supernatants) and cell lysates under both basal and stimulated conditions were collected from WT and KO cells (Fig 4.3A). Immunoblotting analysis of Chromogranin B, a key DCV cargo protein[145], revealed a significant reduction in their secretion from KO cells compared to WT (Fig. 4.3B, 4.3C). WT PC12 cells showed robust secretion upon stimulation, whereas VGF-deficient PC12 clones exhibited significantly reduced stimulus-coupled secretion, indicating impaired regulated release (Fig. 4.3D, 4.3E). This indicated that VGF deficiency affects DCV exocytosis resulting in impaired regulated secretion. These findings establish a mechanistic link between VGF

expression and the efficiency of regulated secretion from DCVs, and implicate VGF as a novel modulator of stimulus-coupled exocytosis in neuroendocrine cells.

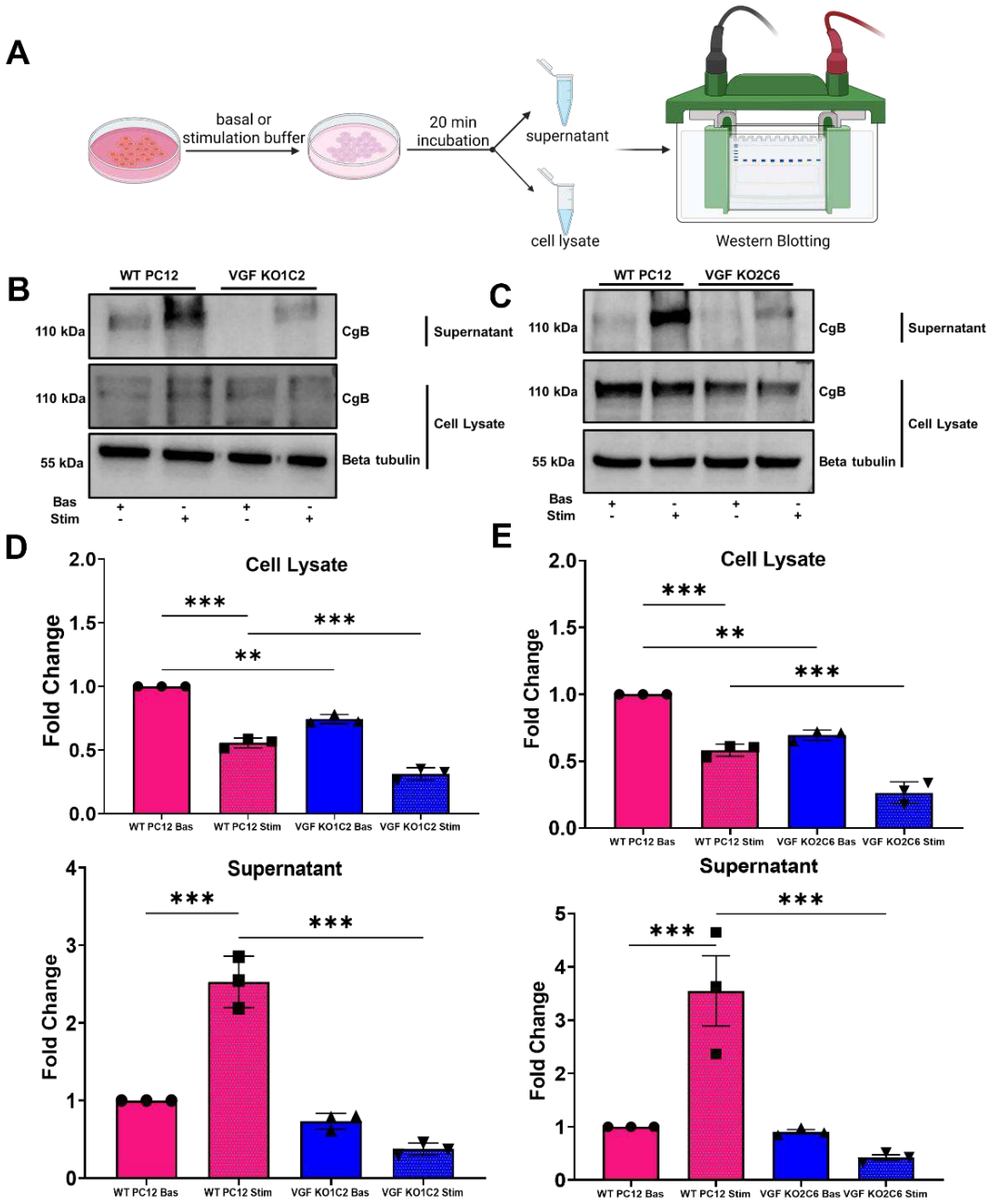

Figure 4.3: Loss of VGF impairs RSP in PC12 Cells. A. Schematic showing the protocol for the stimulus-coupled secretion assay (SCSA). **B.** Representative immunoblots of SCSA in WT PC12 and VGF KO1C2 showing impaired CgB release in WT compared to KO. **C.** Representative immunoblots of SCSA in WT PC12 and VGF KO2C6 showing impaired CgB release in WT compared to KO. **D.** Quantification reveals impaired secretion in CgB levels in KO1C2 upon comparison with WT. **E.** Quantification reveals impaired secretion in CgB levels in KO2C6 upon comparison with WT. n=3, Data shown as mean ± SEM. (*P<0.05, **P<0.01, ***P<0.001; n.s. statistically non-significant).

4.4 Constitutive Secretion remains unaffected in VGF KO cells

To ensure that the observed deficits in stimulus-coupled secretion in VGF KO cells were not due to a general impairment of the secretory machinery, we next examined the status of the constitutive secretory pathway. Unlike regulated secretion, which requires external stimuli such as calcium influx to trigger vesicle fusion, the constitutive pathway operates continuously and is responsible for the unregulated trafficking of proteins to the plasma membrane or extracellular space[27,146]. The overall protein secretion in basal conditions was analysed. WT and KO cells were incubated in Tyrode's basal buffer for 3 hours and the released fractions (supernatants) and cell lysates under basal conditions were collected from WT and KO cells (Fig. 4.4A). As a marker of constitutive secretion, we probed for the molecular chaperone Heat Shock Protein 90 (HSP90) via immunoblotting. HSP90 is known to be released via non-classical, constitutive secretion routes and has been used as a control in previous studies investigating secretion pathways[147,148]. Immunoblot analysis of supernatants from WT and VGF KO cells revealed comparable levels of secreted HSP90, suggesting that basal secretion remained unaffected in the absence of VGF (Fig 4.4B, 4.4E)[139]. To assess whether any changes were observed in the global constitutive signature[137], the cell lysates and supernatants were separated using SDS Page, stained with Coomassie Blue for an hour and subsequently washed to enhance contrast. The gel images were captured using a Gel Doc System and band intensities were analysed (Fig. 4.4C, 4.4D, 4.4F). The results showed no significant differences in the secreted protein levels in WT and KO cells, thus confirming that the absence of VGF does not disrupt the constitutive pathway. Taken together, these results indicate that loss of VGF does not affect the basal, constitutive secretory pathway in PC12 cells. This strongly supports the notion that VGF selectively influences the regulated secretory pathway mediated by DCVs, without perturbing global vesicle trafficking or general secretory competence. These findings are consistent with the known compartmentalization of vesicular trafficking into distinct regulated and constitutive routes in neuroendocrine cells[8,143].

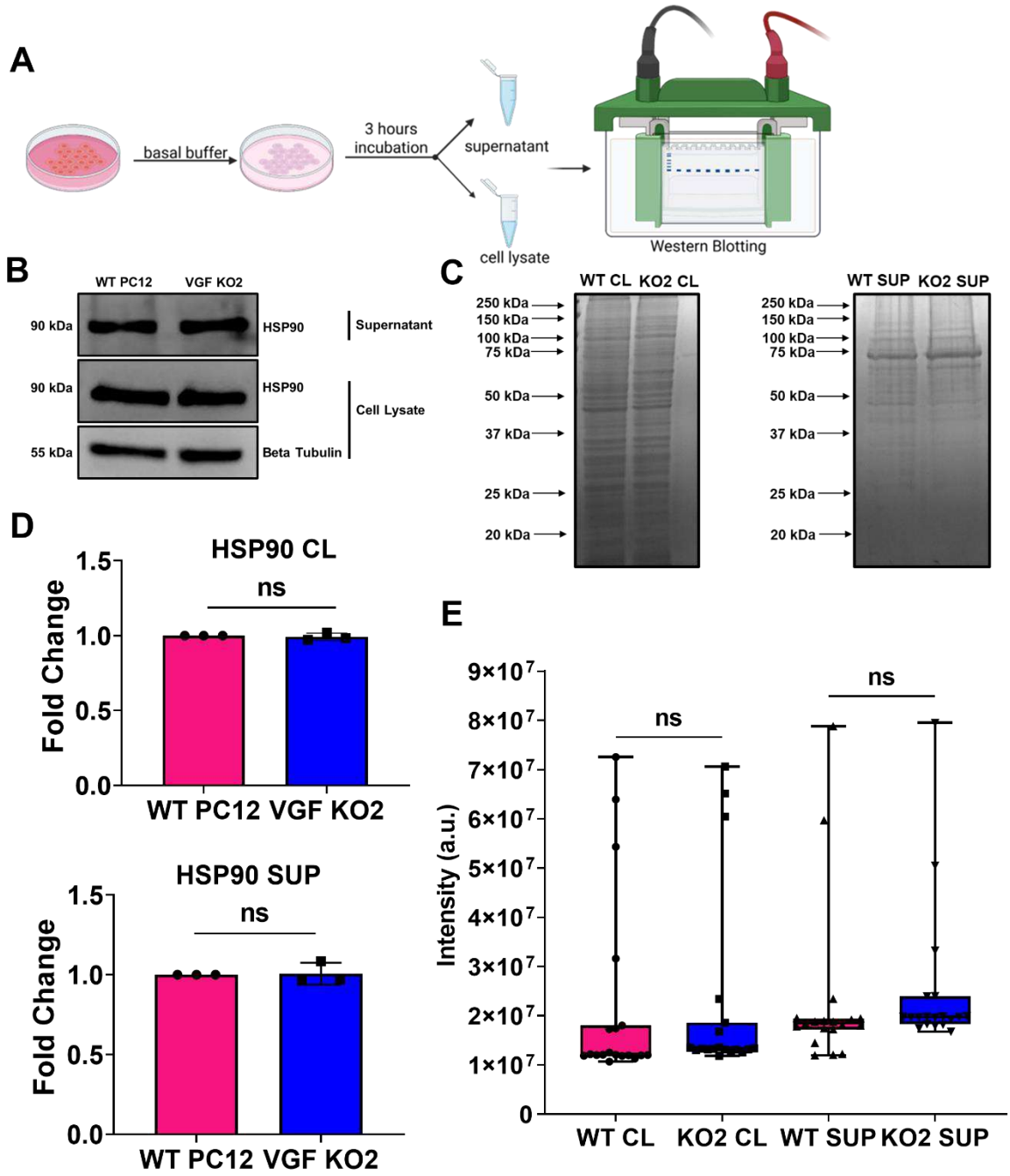

Figure 4.4: Constitutive Secretion is not affected in VGF KO PC12 Cells. A. Schematic showing the protocol for the constitutive assay. **B.** Representative immunoblots of constitutively secreted protein (HSP90) showing comparable levels in both supernatant and cell lysate fractions in WT PC12 and VGF KO2 cells. **C.** Coomassie gel images showing the global constitutive signature in WT and KO2 lysates and supernatants. **D.** Quantification reveals no change in HSP90 levels in VGF KO2 upon comparison with WT. **E.** Quantification considering the auto-detected band intensities using Image-Lab software in WT PC12 and VGF KO2 cells, where each dot represents individual band intensities. n=3. Data is shown as mean ± SEM. (*P<0.05, **P<0.01, ***P<0.001; n.s. statistically non-significant).

4.5 Real time imaging shows compromised DCV Exocytosis

To further validate the secretion impairment, we carried out real time imaging in WT and KO cells using NPY-pHlourin where a pH-sensitive fluorescent reporter (pHlourin) fused to Neuropeptide Y (NPY), a well-established DCV cargo (Fig. 4.5A). pHlourin is a pH-sensitive mutant of green fluorescent protein (GFP) that exhibits a strong increase in fluorescence when exposed to neutral or slightly alkaline pH and is quenched under acidic conditions[149]. This property makes it an ideal reporter for studying vesicle trafficking and exocytosis, especially when fused to proteins that are localized to acidic compartments such as secretory vesicles, endosomes, or synaptic vesicles. In regulated exocytosis, pHlourin is typically fused to the luminal domain of a vesicle-resident or cargo protein. When vesicles are inside the cell, their lumens are acidic (pH ~5.5), and the pHlourin fluorescence is quenched. Upon vesicle fusion during exocytosis, the vesicle lumen is exposed to the neutral pH of the extracellular environment (~7.4), leading to a rapid release of fluorescence[150]. This change can be monitored in real-time using live-cell fluorescence microscopy, allowing for direct visualization and quantification of exocytotic events[151]. One commonly used construct is NPY-pHlourin, where neuropeptide Y (NPY), a dense core vesicle (DCV) cargo protein, is fused to pHlourin. This allows selective labeling of DCVs and enables real-time tracking of their fusion with the plasma membrane during regulated secretion[152]. KCl induces membrane depolarisation, which causes fusion and subsequent exocytosis of DCVs. Upon K+ stimulation, NPY release (indicated by fluorescent puncta) was prominent in WT cells but was significantly reduced in VGF knockout cells demonstrating a marked reduction in both the number and frequency of NPY-pHlourin fusion events, consistent with a defect in the regulated secretory pathway (Fig. 4.5B). As a measure of DCV exocytosis, we quantified the maximum fold change in NPY-pHlourin puncta fluorescence (max df/fo), which shows a significantly diminished release of overall vesicular content in VGF KO cells (Fig 4.5C, 4.5E). There was no significant change observed in the basal fluorescence levels of these cells (Fig. 4.5D). Together, these findings establish that loss of VGF

compromises the regulated secretion machinery in PC12 cells, likely by impairing DCV trafficking, docking, or fusion.

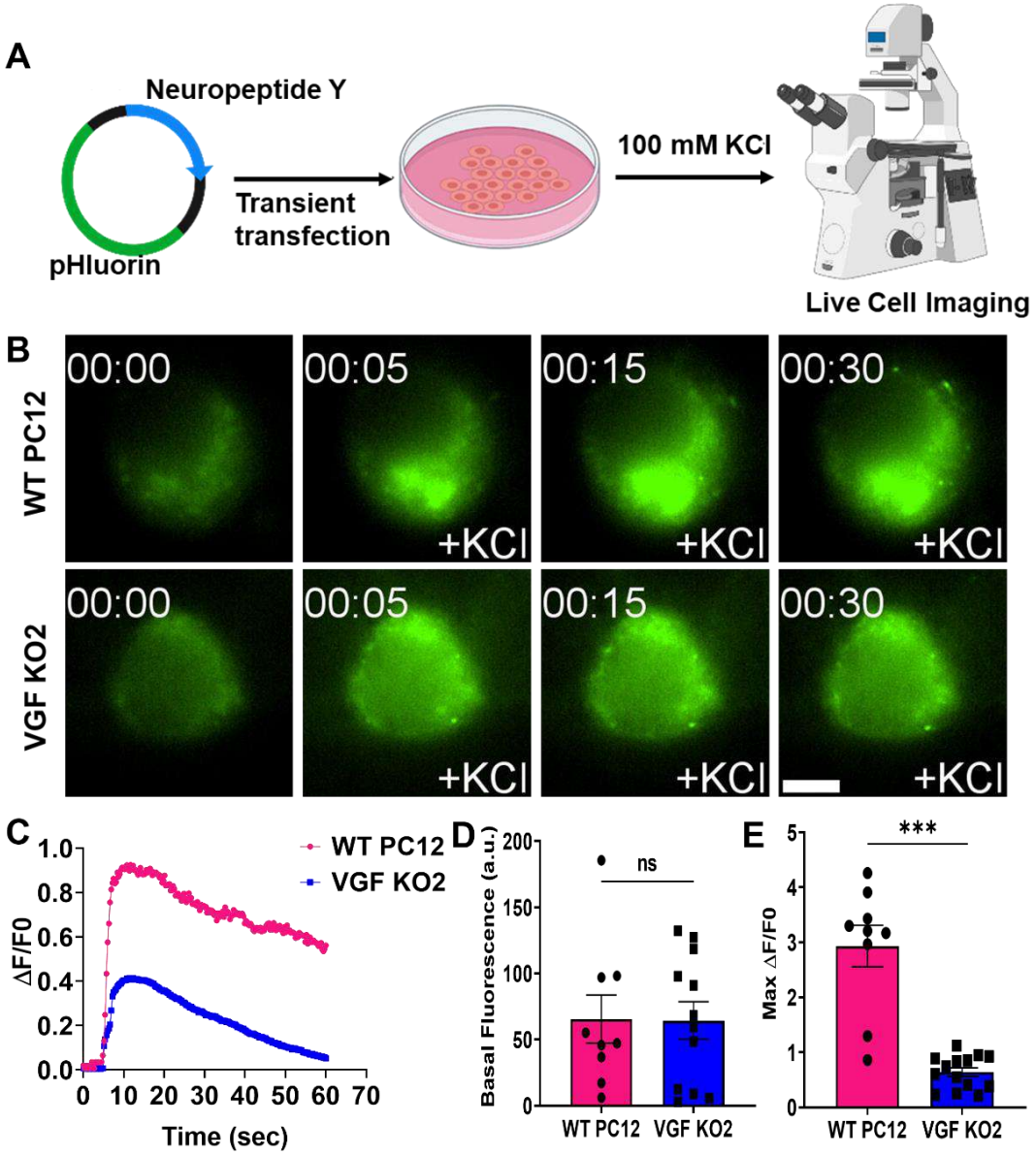

Figure 4.5: Real time imaging shows compromised DCV Exocytosis. A. Schematic showing the protocol for the NPY-pHlourin live cell imaging. **B.** Representative images of WT PC12 and VGF KO2 cells transfected with NPY-pHlourin (green) showing fluorescent intensity change after stimulation. Scale bar 5µm **C.** Representative time traces of mean NPY-pHlourin fluorescence intensities showing an average of all puncta per cell (magenta WT PC12; blue VGF KO2). (N=3). **D.** Quantification of basal intensities shows comparable levels of NPY-pHlourin in WT PC12 (n=8 cells) vs VGF KO2 (n=13 cells). **E.** Quantitative analysis of the maximum Δf/f0 in WT PC12 (n=8 cells) and VGF KO2 cells (n=13 cells). (Mann-Whitney Test). ('N' denotes the number of independent experiments, and 'n' is the number of cells taken for quantification). Data are shown as mean ± SEM. (*P<0.05, **P<0.01, ***P<0.001; n.s. statistically non-significant).

4.6 Overexpression of VGF shows Partial Restoration of Regulated Exocytosis

To ascertain that the observed impairment in stimulus-coupled DCV exocytosis in VGF KO cells was specifically attributable to the absence of VGF, a rescue experiment was conducted by overexpressing the VGF gene. VGF KO cells were transiently transfected with a plasmid encoding full-length rat VGF tagged at the N-terminus with GFP, enabling both expression tracking and functional rescue assessment. Following this, cells were subjected to a real-time live-cell secretion assay using a fluorescently tagged DCV cargo, Neuropeptide Y (NPY) fused to pH-sensitive Tomato fluorescent protein (NPY-pHTomato)[153,154]. This reporter allows detection of exocytosis events in real-time, as the fluorescence of pH-sensitive Tomato increases upon exposure to the neutral extracellular pH during DCV fusion with the plasma membrane. Stimulation was induced using high-potassium (100 mM KCl) depolarization buffer, a well-established method to elicit calcium influx and trigger regulated secretion[155,156]. KCl induces membrane depolarisation, which causes fusion and subsequent exocytosis of DCVs. Live-cell imaging was performed and fluorescence changes corresponding to vesicle fusion were captured over time (Fig. 4.6A). Upon K+ stimulation, partial restoration of exocytosis was observed in the rescue condition as seen by an increased number of NPY-pH tomato fusion events compared to the KO condition (Fig. 4.6B). Quantitative analysis revealed that although the number of exocytotic events did not reach WT levels, the Rescue condition demonstrated a statistically significant restoration in regulated secretion of DCVs (Fig. 4.6C, 4.6E). This partial rescue suggests that VGF overexpression is sufficient to support functional recovery of DCV exocytosis. Importantly, basal fluorescence intensity, which corresponds to the resting state of DCVs in the absence of stimulation, remained unchanged between the WT, KO and Rescue conditions (Fig. 4.6D). This finding indicates that the increase in fluorescence upon depolarization was due to bonafide exocytotic fusion events rather than differences in vesicle loading, expression levels, or basal trafficking. These results strongly support our hypothesis that VGF plays a direct and functional role in facilitating regulated exocytosis via the dense-core vesicle pathway in PC12 cells. The ability of VGF overexpression to restore exocytotic capacity further validates the specificity of the phenotype observed in VGF KO cells and highlights

the importance of VGF in the molecular machinery governing neuroendocrine secretion.

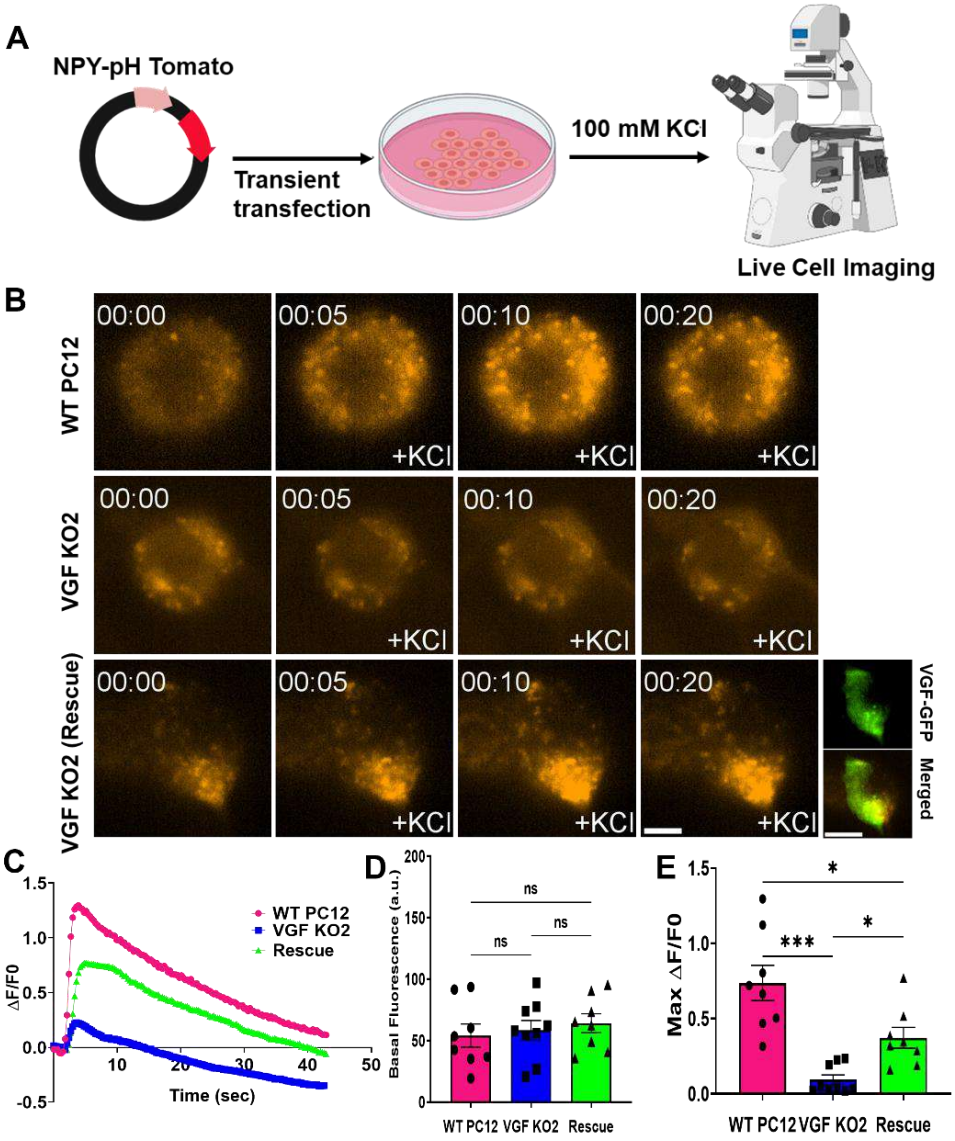

Figure 4.6: Rescue experiments reveal partial restoration of Regulated Exocytosis. **A.** Schematic showing the protocol for the NPY-pH tomato live cell imaging. **B.** Representative images of WT PC12, VGF KO2 and VGF KO2 (Rescue) cells transfected with NPY-pH tomato (red) and VGF GFP (green, in case of rescue) showing fluorescent intensity change after stimulation. Scale bar 5µm. **C.** Representative time traces of mean NPY-pH tomato fluorescence intensities showing an average of all puncta per cell (magenta WT PC12; blue VGF KO2, green VGF KO2 (Rescue)) (N=3). **D.** Quantification of basal intensities shows comparable levels of NPY-pH tomato in WT PC12 (n=8 cells), VGF KO2 (n=9 cells) and VGF KO2 (Rescue) (n=8 cells). **E.** Quantitative analysis of the maximum Δf/f0 in WT PC12 (n=8 cells), VGF KO2 cells (n=9 cells) and VGF KO2 (Rescue) (n =8 cells). (Mann-Whitney Test). ('N' denotes the number of independent experiments, and 'n' is the number of cells taken for quantification). Data are shown as mean ± SEM. (*P<0.05, **P<0.01, ***P<0.001; n.s. statistically non-significant).

4.7 Release of Synaptic like Vesicles is not altered in VGF KO Cells

Traditionally, VGF has been characterized as a member of the Granin family and implicated primarily in the biogenesis, cargo sorting, and regulated exocytosis of DCVs, which are essential for the activity-dependent secretion of neuropeptides and hormones in neuroendocrine and neuronal cells[157]. To determine whether the absence of VGF also affects the trafficking of other secretory compartments such as synaptic-like vesicles (SLVs), we employed live-cell imaging using Synaptophysin-pHlourin, a pH-sensitive fluorescent reporter system. Synaptophysin, a canonical marker of SLVs, was fused to pHlourin, a pH-sensitive GFP variant allowing real-time visualization of SLV exocytosis upon KCl induced stimulation[158] (Fig. 4.7A). Upon K+ stimulation, no significant difference was observed in Synaptophysin release (indicated by fluorescent puncta) in the WT and KO cells (Fig. 4.7B). Quantitative analysis of the fluorescence signal showed that the maximum change in fluorescence intensity ($\Delta F/F_0$) was comparable between WT and KO cells, indicating no impairment in SLV release dynamics (Fig. 4.7C, 4.7E). Furthermore, baseline fluorescence levels prior to stimulation were not significantly different, suggesting that SLV biogenesis, trafficking, or vesicle loading remained unaltered in the absence of VGF (Fig. 4.7D). These findings indicate that the loss of VGF selectively impairs the DCV-mediated regulated secretory pathway, without affecting SLV-mediated neurotransmitter release mechanisms. This specificity implies the functional compartmentalisation of VGF and aligns with previous reports that VGF-derived peptides are sorted into DCVs and are absent from synaptic vesicles[1,20]. These results ensure that VGF is a dedicated regulator of DCV cargo processing, trafficking, or release, with no detectable role in the SLV machinery.

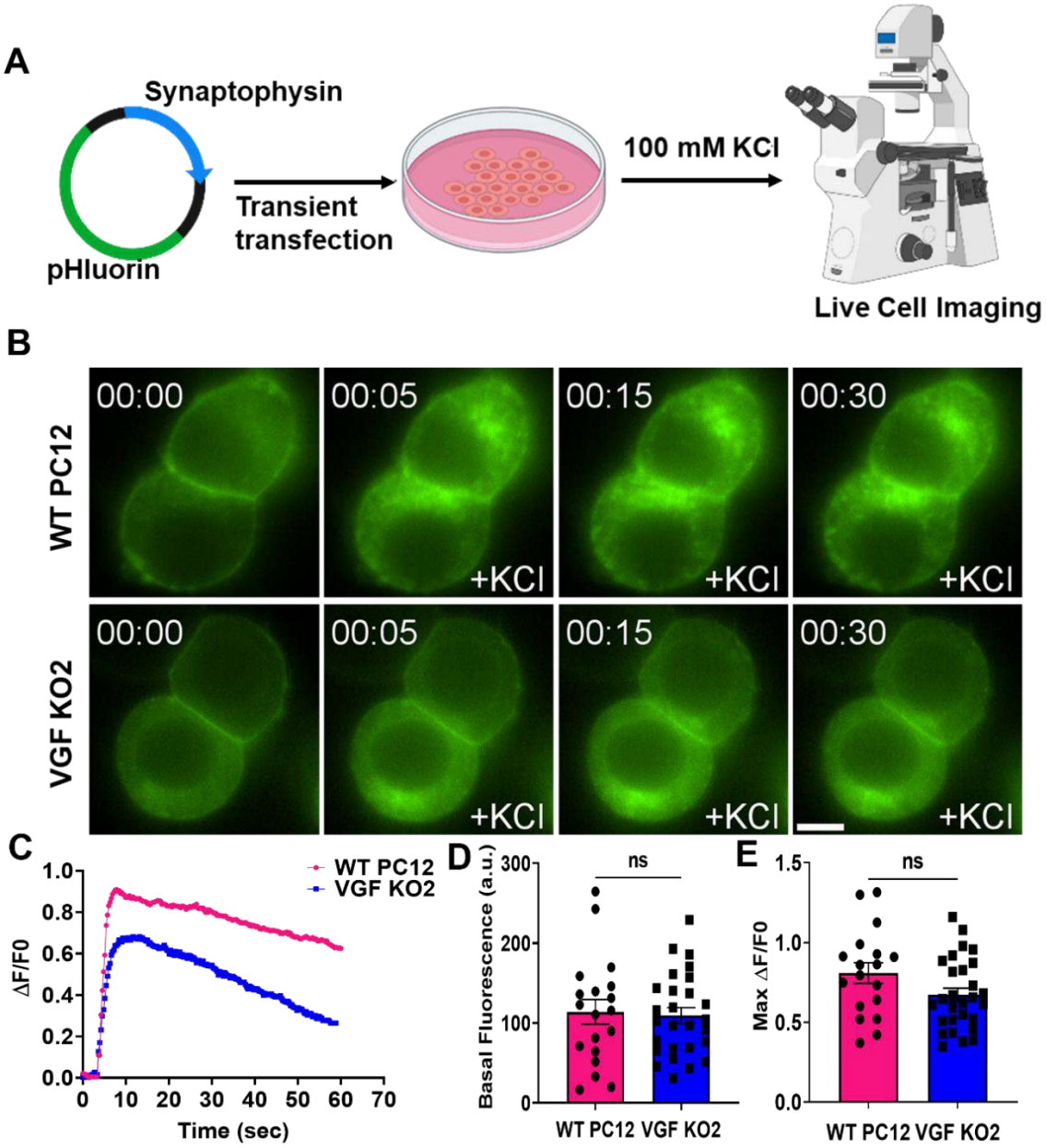

Figure 4.7: Release of synaptic-like vesicles is not altered in VGF KO cells. A. Schematic showing the protocol for the Synaptophysin-pHlourin live cell imaging. **B.** Representative images of WT PC12 and VGF KO2 cells transfected with Synaptophysin-pHlourin (green) showing fluorescent intensity change after stimulation. Scale bar 5µm. **C.** Representative time traces of mean Synaptophysin-pHlourin fluorescence intensities showing an average of all puncta per cell (magenta WT PC12; blue VGF KO2). (N=3). **D.** Quantification of basal intensities shows comparable levels of Synaptophysin-pHlourin in WT PC12 vs VGF KO2 (n=15 cells). **E.** Quantitative analysis of the maximum Δf/f0 in WT PC12 and VGF KO2 cells (n=18 cells). (Mann-Whitney Test). ('N' denotes the number of independent experiments, and 'n' is the number of cells taken for quantification). Data are shown as mean ± SEM. (*P<0.05, **P<0.01, ***P<0.001; n.s. statistically non-significant).

4.8 Super-resolution imaging reveals altered vesicle morphology but preserved biogenesis in VGF KO Cells

To investigate whether the impaired regulated secretion observed in VGF KO cells arise from defects in DCV morphology, we employed super-resolution Stimulated Emission Depletion (STED) microscopy, which enables imaging at sub-diffraction limit resolution (~40–70 nm), thereby allowing precise visualization of vesicle size and distribution[134]. Cells were immunostained for Secretogranin II (ScgII), a Granin family member abundantly localized in DCVs and widely used as a molecular marker for this vesicle population[19]. ScgII also plays a role in prohormone sorting and vesicle condensation at the TGN, thus serving as a robust indicator of both vesicle presence and functional integrity[18]. Quantitative image analysis of STED revealed that the total number of ScgII positive vesicles per cell did not significantly differ between WT and VGF KO conditions (Fig. 4.8A, 4.8B). This suggests that vesicle biogenesis and overall formation of DCVs are not grossly impaired by the loss of VGF[14,15]. These findings are consistent with previous studies showing that granins, including ScgII, facilitate but are not solely responsible for vesicle budding and biogenesis, which primarily involves core trafficking machinery including AP-1, PACS-1, and various sorting receptors[81,159]. This indicates that the core machinery responsible for vesicle generation at the trans-Golgi network (TGN) remains functional in the absence of VGF. However, detailed morphometric analysis of the vesicle size distribution revealed a pronounced shift toward smaller vesicles in VGF KO cells. Specifically, the proportion of vesicles with diameters less than 150 nm was significantly increased in KO cells relative to WT, which typically displayed a broader size distribution, including larger vesicles (150–250 nm) (Fig. 4.8C). This size reduction may reflect impaired vesicle maturation, defective condensation of cargo, or altered fusion and budding dynamics, all of which are processes in which Granin family members, particularly VGF are reported to participate[1,160]. Given that vesicle size is often correlated with functional competence, larger vesicles being associated with fully matured and docked DCVs this observation may explain the secretory deficits observed in VGF deficient cells. Moreover, smaller vesicles may indicate inefficient recruitment of peptide/protein cargoes, a phenomenon observed in other Granin or DCV component knockouts[104,138]. Collectively, these results suggest that while initial DCV biogenesis is not dependent on VGF, the maturation,

proper condensation, and expansion of vesicular compartments may be compromised in its absence, potentially accounting for the observed defects in regulated secretion. However, to definitively determine whether defects in vesicle maturation or docking underlie the observed phenotypes, future studies employing high-resolution ultrastructural analysis using transmission electron microscopy (TEM) will be necessary.

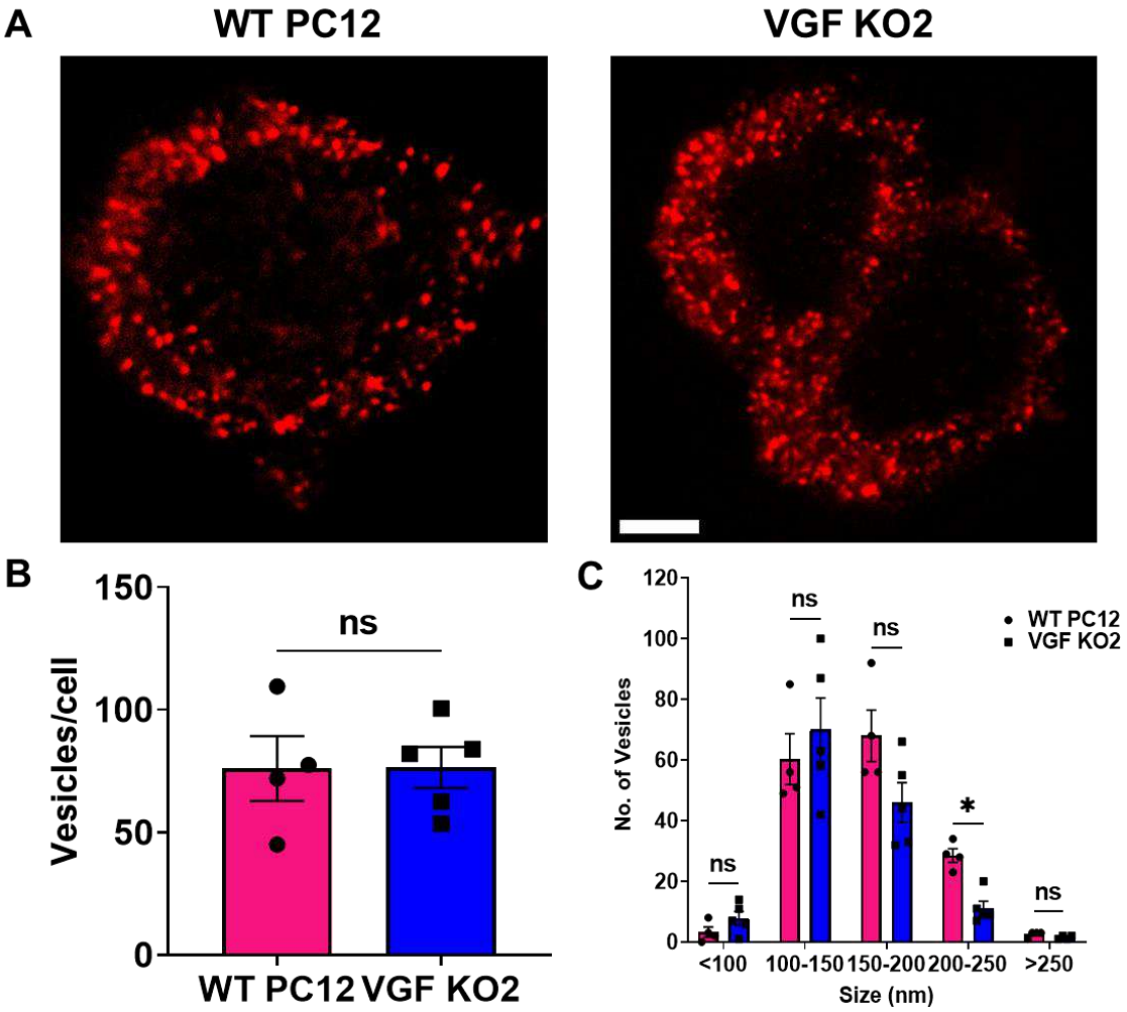

Figure 4.8: STED imaging reveals altered vesicle morphology but preserved biogenesis in VGF KO cells. A. Representative STED images of WT PC12 and VGF KO2 cells. Scale bar 5 µm. **B.** Quantification reveals no significant difference in the number of vesicles per cell, where each dot represents one image. **C.** Morphometric analysis of the vesicle size distribution reveals a shift towards smaller vesicles (<150nm) in VGF KO2 (blue) while the WT PC12 cells (magenta) showed a broader size distribution. (N=1, n=9 cells each). ('N' denotes the number of independent experiments, and 'n' is the number of cells taken for quantification). Data are shown as mean ± SEM. (*P<0.05, **P<0.01, ***P<0.001; n.s. statistically non-significant).

4.9 VGF KO impairs Full Fusion Exocytosis without affecting Kiss-and-Run Events

Regulated exocytosis in neuroendocrine cells operates primarily via two distinct modes: kiss-and-run and full fusion. In kiss-and-run exocytosis, secretory vesicles transiently fuse with the plasma membrane, forming a narrow, reversible fusion pore that permits partial cargo release before the vesicle detaches and recycles. In contrast, full fusion entails a complete merger of the vesicle membrane with the plasma membrane, resulting in full cargo discharge and membrane incorporation[161]. These two modes can be discriminated based on the size of the fusion pore that is formed during the exocytic event. Specifically, 10 kDa dextran molecules, which can pass through ~5 nm pores, are able to enter vesicles during kiss-and-run events. In contrast, 40 kDa dextrans, which require ~9 nm pores, can only enter through full fusion events[21,162,163]. To investigate whether VGF influences specific exocytosis modes, we performed a dextran uptake assay using rhodamine-conjugated 10 kDa and 40 kDa dextrans in both WT and VGF KO cells. Cells were stimulated under depolarizing conditions using 100 mM KCl for 5 minutes to promote calcium-dependent vesicle fusion and dextran uptake. Under these conditions, dextran can be taken up via either kiss-and-run or full fusion events. Quantitative fluorescence analysis revealed that uptake of 10 kDa dextran was comparable between WT and VGF KO cells (Fig. 4.9A-C), suggesting that the frequency or efficiency of kiss-and-run exocytic events remains unaltered in the absence of VGF. However, in comparison to the WT cells, the VGF KO cells exhibited a notable decrease in 40 kDa dextran uptake, suggesting a deficit in full fusion exocytosis (Fig. 4.9D-F). These results suggest that VGF is required for efficient formation or stabilisation of the larger fusion pores associated with full fusion, but not for the transient, smaller pore dynamics of kiss-and-run. Previous studies have shown that full fusion events are often associated with matured vesicles that are fully loaded with neuropeptides and exhibit appropriate membrane curvature and lipid composition to support pore dilation[153]. Loss of VGF may disrupt one or more of these processes, leading to vesicles that fail to undergo full fusion despite being capable of initiating kiss-and-run fusion. Collectively, these findings demonstrate that VGF plays a selective and critical role in enabling full fusion exocytosis, possibly by promoting proper vesicle maturation or membrane dynamics required for wide-pore formation.

4.10 VGF KO leads to delayed clearance of endocytic cargo, suggesting disruption in Endolysosomal Trafficking

One of the more intriguing and unanticipated findings of this study was the delayed clearance of 10 kDa fluorescent dextran observed in VGF KO PC12 cells. Cells were labelled with Alexa Fluor rhodamine conjugated 10 kDa dextran and subsequently chased for 6 hours (Fig. 4.9G). In contrast to WT cells, which exhibited efficient clearance of dextran-positive puncta indicative of normal Endolysosomal processing, KO cells retained a substantial number of fluorescent puncta, signifying delayed or impaired trafficking through the Endolysosomal pathway (Fig. 4.9H). This result implies that VGF may play a role in the post-exocytotic fate of secretory vesicles or the homeostasis of vesicle recycling machinery. Normally, after full fusion exocytosis, components of secretory vesicles are retrieved and either recycled back to the trans-Golgi network or targeted to late endosomes/lysosomes for degradation or remodelling[164]. The persistent retention of dextran in KO cells suggests a disruption in vesicle-endosome-lysosome fusion events, trafficking delays, or impaired degradation processes.

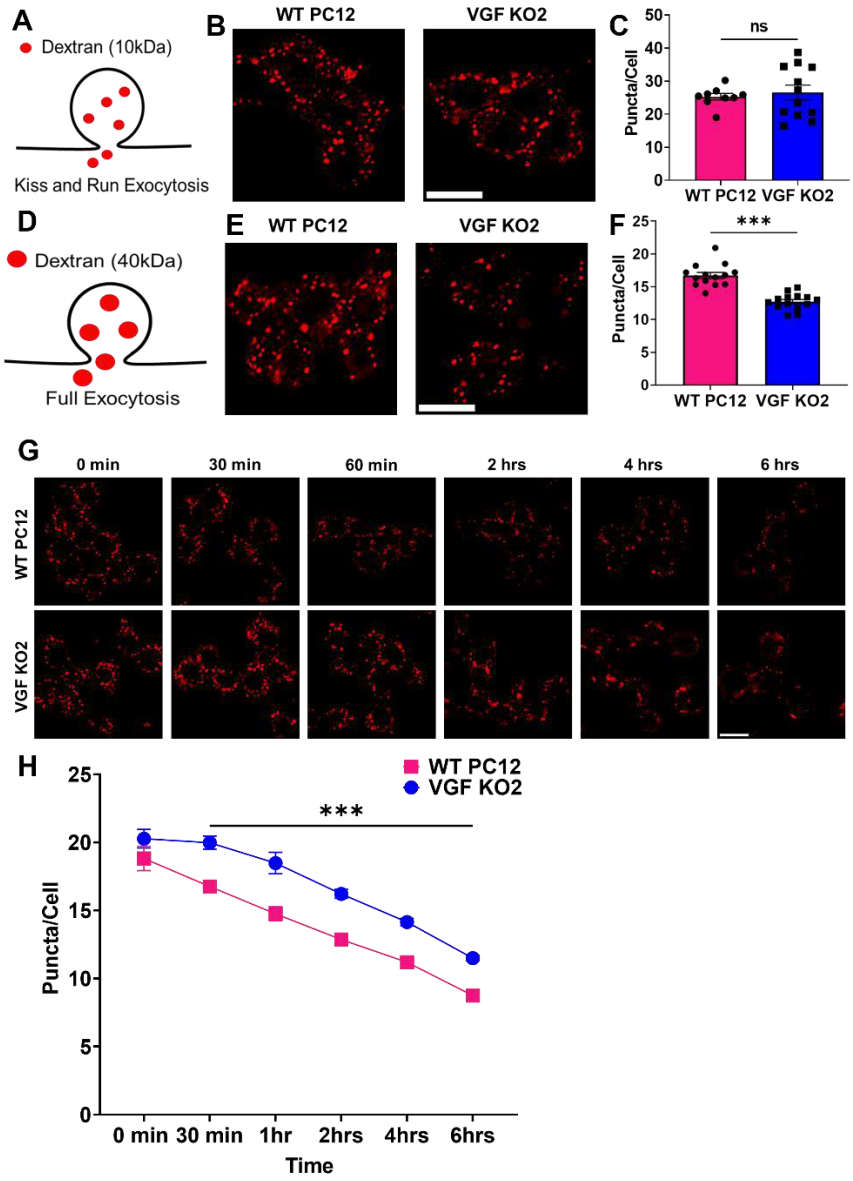

Figure 4.9: VGF KO impairs full fusion exocytosis as well as Endolysosomal clearance. A. Schematic for the kiss-and-run exocytotic events. **B-C.** Representative images and quantification for Dextran 10kDa show no significant changes in WT PC12 (magenta) vs VGF KO2 (blue). (N=3, n=13 cells each). Scale bar 5µm **D.** Schematic for the full fusion exocytotic events. **E-F.** Representative images and quantification for Dextran 40kDa show impaired full fusion exocytosis as the puncta per cell reduces in VGF KO2 cells (blue) w.r.t. WT PC12 cells (magenta). (N=3, n=13 cells each). **G-H.** Representative confocal images and quantification for the Endolysosomal assay using Dextran 10kDa shows a defect in the clearance of the dextran puncta till 6 hours of chase in VGF KO2 (blue) w.r.t. WT PC12 cells (magenta). Scale bar 5µm. (N=3, n=10 cells each). ('N' denotes the number of independent experiments, and 'n' is the number of cells taken for quantification). Data are shown as mean ± SEM. (*P<0.05, **P<0.01, ***P<0.001; n.s. statistically non-significant).

Chapter 5
Discussion

Chapter 5

Discussion

Neuroendocrine secretion is a highly regulated process that depends on the biogenesis, maturation, trafficking, and exocytosis of DCVs[165]. VGF, a member of the Granin family, has been known for a long time to be sorted into DCVs, but its exact functional role was not clear[1]. By a broad series of experiments with VGF KO cells, we present strong evidence that VGF is essential and specific for regulated secretion by DCVs, but does not affect constitutive or SLV trafficking. Our results clarify a multi-faceted function for VGF in DCV maturation, full-fusion exocytosis, and post-exocytic vesicle processing, thus establishing VGF as an important regulator of neuroendocrine vesicular dynamics. Early characterisation of the VGF KO cells identified a significant defect in stimulus-coupled exocytosis of DCV cargo. Real-time imaging using NPY-pHlourin indicated highly reduced depolarisation-evoked fusion events and reduced vesicular release (Fig. 4.5), which indicates that VGF is critical for regulated DCV exocytosis. This was also confirmed by recovery of exocytotic capability upon overexpression of VGF in the KO cells (Fig. 4.6), which restored fusion events to almost WT levels, demonstrating the specificity of the defect to the depletion of VGF. Notably, the constitutive secretion pathway was unaffected, as revealed by comparable secretion of HSP90 with WT cells and similar Coomassie-stained secretome profiles (Fig. 4.4). These findings highlight that the loss of VGF is not globally inhibitory for vesicle trafficking or secretion but specifically targets the stimulus-dependent regulated pathway particular to DCVs. This differential impairment is consistent with earlier descriptions of functional compartmentalisation of secretory pathways in neuroendocrine cells[8,62], where the Granin family, such as VGF, which is largely confined to DCVs and not found in constitutive or synaptic vesicle compartments[1,18]. Despite VGF's Granin origin and its localisation in DCVs, it was essential to check if VGF also influenced other secretory organelles. As a live reporter for SLVs, Synaptophysin-pHlourin was used here, and we observed no variation in the release dynamics of SLVs between WT and KO cells (Fig. 4.7). This finding supports that VGF specifically regulates DCV function rather than overall mechanisms of exocytosis. These findings confirm

reports that VGF-derived peptides are sorted only into DCVs and not into SLVs[1,142], highlighting a specialized function for VGF in neuropeptide storage and release. Although the DCV numbers tagged by ScgII were not significantly different between WT and KO cells (Fig. 4.8), morphometric analysis of vesicle size by STED microscopy indicated that there was a shift toward smaller vesicles in VGF-deficient cells. This might imply that VGF is not necessary for vesicle biogenesis as such, but could be important for maturation of the vesicles, which involves cargo condensation, acidification of the lumen, and membrane shaping[104,160]. Smaller vesicles might lack the capability for complete loading of the cargo or efficient fusion, which can account for the diminished exocytosis. Moreover, to establish the fact that there is a defect in docking and maturation of vesicles, additional Ultrastructural analysis must be conducted through Transmission Electron Microscopy (TEM). Additional functional analysis by dextran uptake assays also suggested that VGF KO cells are still capable of kiss-and-run exocytosis as shown by intact uptake of 10 kDa dextran but with a particular deficiency in full fusion events, as 40 kDa dextran uptake was affected (Fig. 4.9). Successful full fusion involves accurate membrane curvature, vesicle maturation, and coordination by the cytoskeleton[40,163], all of which could be disrupted in absence of VGF. The capacity to perform kiss-and-run but not full fusion also supports a pore dilation or stabilization role for VGF, which is in keeping with its suggested roles in vesicle maturation and fusion pore opening[162]. A novel observation in this study is the delayed clearance of dextran from VGF KO cells after chase experiments for 6 hours (Fig. 4.9). Although this may be due to defective lysosomal breakdown or endosomal merging, it opens the possibility that VGF could also control trafficking processes subsequent to exocytosis[166]. Following complete fusion, vesicle membranes are usually recovered and recycled or degraded through the Endolysosomal pathway[164]. The accumulated dextran puncta in VGF KO cells indicate that VGF loss might disrupt these mechanisms. A number of arguments in the literature demonstrate that proteins required for DCV maturation and exocytosis are also closely connected with Endolysosomal trafficking regulation. Chromogranin A (CgA), another Granin family protein, has been demonstrated to control membrane budding and trafficking from the TGN and can impact multiple functions of lysosomes when dysregulated[50]. Likewise, Secretogranin III is recognised to interact with cholesterol-rich microdomains that are important for cargo sorting and stabilisation of vesicles[108]. With these precedents VGF or its

peptides are likely involved in sorting signals or structural integrity for efficient cargo handoff between degradative and secretory compartments. Additionally, recent studies have attributed neuropeptides and their precursors to Endolysosomal homeostasis and regulation of autophagy[167]. VGF-derived peptides like TLQP-21 have been found to influence vesicle trafficking as well as energy homeostasis pathways[2]. Hence, the lack of VGF might influence not only exocytotic activity but also post-fusion vesicle resolution, recycling, or degradation, leading to the accumulation of non-processed cargo or vesicles that can impair secretory capacity in the long term. Such interruptions in the Endolysosomal process might result in cellular stress, changed organelle structure, and defective secretion, consequently influencing neuroendocrine signalling. Delayed cargo clearance could also point to defective lysosome biogenesis or acidification, both of which are essential for the degradation of the cargo. Although our findings do not as yet directly point to the trafficking stage implicated, they reveal a new and significant function for VGF in ensuring the dynamic turnover and stability of the secretory and Endolysosomal pathways. Together, our findings provide a comprehensive overview of VGF as an atypical and selective regulator of the dense-core secretory pathway. Mechanistically, VGF could interact with other granins or retention machinery and membrane fusion-related vesicle-associated proteins. Future studies employing co-immunoprecipitation and proximity labelling would be able to determine VGF interacting partners in the DCV network. In addition, ultrastructural examination by transmission electron microscopy will be important to determine unequivocally vesicle docking, states of maturation, and membrane organisation in VGF KO cells. Finally, in vivo examination of neuroendocrine tissues or behavioural phenotypes in VGF knockout models would illuminate the physiological significance of these observations in neuropeptide-mediated signalling.

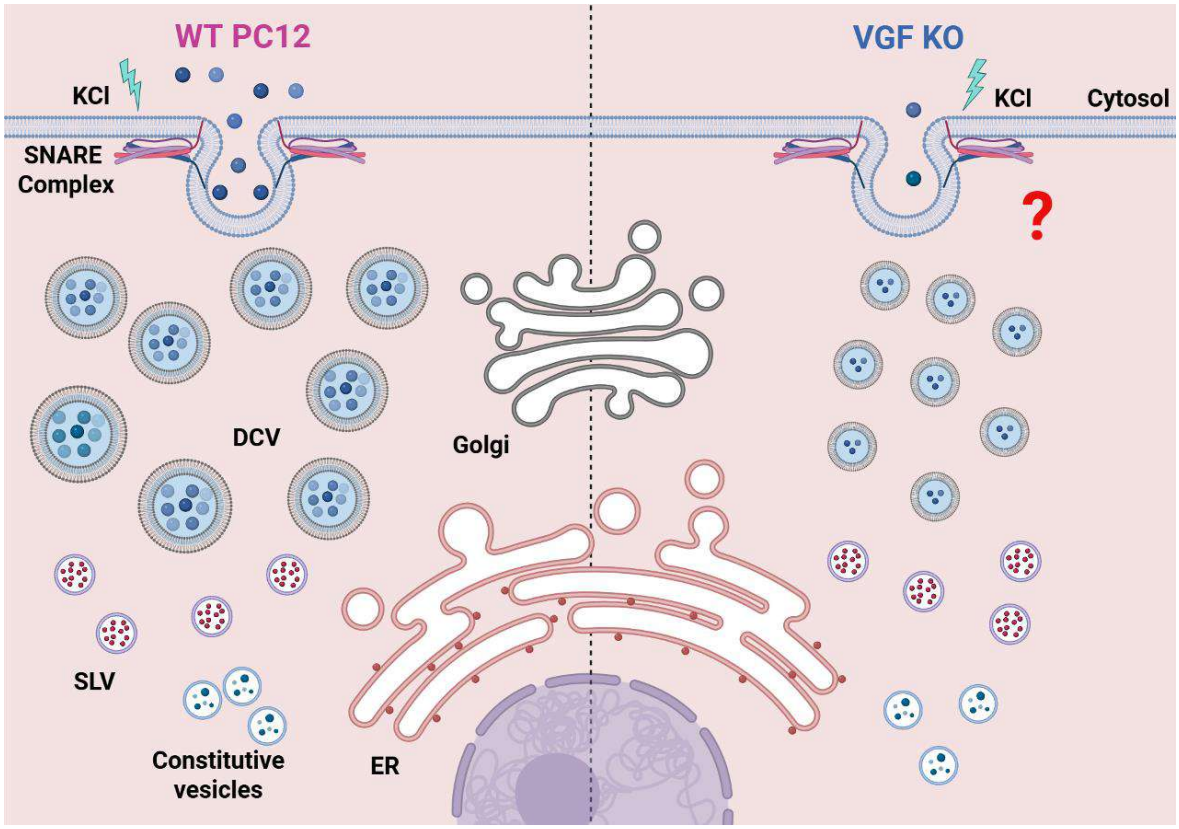

Figure 5.1. Schematic Representation of impaired RSP in VGF-deficient cells.

Concluding Remarks

This study reveals a specific and critical role for VGF in the regulated exocytosis of DCVs in PC12 cells. While CSP and SLV Exocytosis remain unaffected, VGF knockout results in defective stimulus-coupled DCV exocytosis, impaired full-fusion events, and altered vesicle distribution, as shown by pHlourin assays and STED microscopy. Though vesicle number is not hindered, VGF-deficient cells exhibit smaller, likely immature vesicles and signs of disrupted post-exocytic trafficking, possibly linked to Endolysosomal dysfunction. The restoration of secretory function upon VGF overexpression confirms its specificity and essential role in DCV dynamics. These findings establish VGF as a selective regulator of neuroendocrine vesicular trafficking.

Future Directions

To reveal the **mechanistic function of VGF** in DCV biogenesis, trafficking, and secretion, an integrative, multi-faceted strategy could be used which would include, ultrastructural analysis, molecular profiling, and protein interaction studies. First, **Retention Using Selective Hook (RUSH) system** can be used to **dynamically visualize** and obtain **temporal data on DCV cargo trafficking** in VGF KO cells, allowing us to identify **potential defects** in **cargo sorting** in **vesicles and transpor**t. To further investigate whether VGF loss affects dynamic Golgi organisation, **brefeldin A (BFA) treatment** could be used to assess **Golgi integrity and reassembly dynamics**, to test defects in **fragmentation and recovery** in VGF-depleted cells. Based on the detected defects in Endolysosomal trafficking in VGF KO cells, the **dynamic behaviour of endosomal** and **lysosomal compartments** by immunocytochemistry using fluorescent markers like **Rab5, Rab7, LAMP1, and Rab11** could be examined. The measurement of **autophagic flux** and **lysosomal degradation capacity** using LC3-I/II and p62 turnover could also suggest possible functional **impairments in cargo processing**. Following this, **ultrastructural analysis by TEM** will enable us to comment on **defects in vesicle maturation, docking at the plasma membrane,** and **alterations in secretory organelles**. To determine the **molecular basis of defective exocytosis**, the expression, subcellular localisation, and functionality of essential **SNARE complex constituents** like SNAP-25, VAMP-2, and Syntaxin-1 in VGF KO cells could be analysed. Lastly, screening for putative **VGF-interacting proteins** by **co-immunoprecipitation** could be done, followed by **mass spectrometry** to identify **novel molecular partners** and signalling pathways implicated in the biogenesis of vesicles and regulated secretion. Together, these approaches have the potential to provide a comprehensive understanding of the **cellular and molecular mechanisms** by which VGF modulates DCV trafficking and neuroendocrine secretion.

References

1. Salton, S. R. J. *et al.* VGF: A Novel Role for This Neuronal and Neuroendocrine Polypeptide in the Regulation of Energy Balance. *Front. Neuroendocrinol.* **21**, 199–219 (2000).
2. Bartolomucci, A. *et al.* TLQP-21, a VGF-derived peptide, increases energy expenditure and prevents the early phase of diet-induced obesity. *Proc. Natl. Acad. Sci.* **103**, 14584–14589 (2006).
3. Huttner, W. B., Gerdes, H. H. & Rosa, P. The granin-(chromogranin/secretogranin) family. *Trends Biochem. Sci.* **16**, 27–30 (1991).
4. Lewis, J. E., Brameld, J. M. & Jethwa, P. H. Neuroendocrine Role for VGF. *Front. Endocrinol.* **6**, 3 (2015).
5. Thakker-Varia, S. & Alder, J. Neuropeptides in depression: Role of VGF. *Behav. Brain Res.* **197**, 262–278 (2009).
6. Greene, L. A. & Tischler, A. S. Establishment of a noradrenergic clonal line of rat adrenal pheochromocytoma cells which respond to nerve growth factor. *Proc. Natl. Acad. Sci.* **73**, 2424–2428 (1976).
7. Multiplex Genome Engineering Using CRISPR/Cas Systems | Science. https://www.science.org/doi/10.1126/science.1231143.
8. Tooze, S. A., Martens, G. J. M. & Huttner, W. B. Secretory granule biogenesis: rafting to the SNARE. *Trends Cell Biol.* **11**, 116–122 (2001).
9. Mellman, I. ENDOCYTOSIS AND MOLECULAR SORTING. *Annu. Rev. Cell Dev. Biol.* **12**, 575–625 (1996).
10. Billaud, M. *et al.* Regulation of Cellular Communication by Signaling Microdomains in the Blood Vessel Wall. *Pharmacol. Rev.* **66**, 513–569 (2014).
11. Burgoyne, R. D., Helassa, N., McCue, H. V. & Haynes, L. P. Calcium Sensors in Neuronal Function and Dysfunction. *Cold Spring Harb. Perspect. Biol.* **11**, a035154 (2019).
12. Toni, R. The neuroendocrine system: organization and homeostatic role. *J. Endocrinol. Invest.* **27**, 35–47 (2004).
13. Wendler, F., Page, L., Urbé, S. & Tooze, S. A. Homotypic Fusion of Immature Secretory Granules During Maturation Requires Syntaxin 6. *Mol. Biol. Cell* **12**, 1699–1709 (2001).
14. Bonnemaison, M. L., Eipper, B. A. & Mains, R. E. Role of Adaptor Proteins in Secretory Granule Biogenesis and Maturation. *Front. Endocrinol.* **4**, (2013).
15. Kim, T., Gondré-Lewis, M. C., Arnaoutova, I. & Loh, Y. P. Dense-Core Secretory Granule Biogenesis. *Physiology* **21**, 124–133 (2006).
16. Sorting Ourselves Out: Seeking Consensus on Trafficking in the Beta-Cell - Arvan - 2004 - Traffic - Wiley Online Library. https://onlinelibrary.wiley.com/doi/full/10.1111/j.1600-0854.2004.00152.x.
17. Tsuboi, T., McMahon, H. T. & Rutter, G. A. Mechanisms of Dense Core Vesicle Recapture following "Kiss and Run" ("Cavicapture") Exocytosis in Insulin-secreting Cells*. *J. Biol. Chem.* **279**, 47115–47124 (2004).
18. Bartolomucci, A. *et al.* The Extended Granin Family: Structure, Function, and Biomedical Implications. *Endocr. Rev.* **32**, 755–797 (2011).
19. Taupenot, L., Harper, K. L. & O'Connor, D. T. The Chromogranin–Secretogranin Family. *N. Engl. J. Med.* **348**, 1134–1149 (2003).
20. Ferri, G.-L. & Possenti, R. *vgf* A neurotrophin-inducible gene expressed in neuroendocrine tissues. *Trends Endocrinol. Metab.* **7**, 233–239 (1996).
21. Journal of Comparative Neurology | Systems Neuroscience Journal | Wiley Online Library. https://onlinelibrary.wiley.com/doi/abs/10.1002/%28SICI%291096-9861%2819980427%29394%3A1%3C91%3A%3AAID-CNE7%3E3.0.CO%3B2-C?sid=nlm%3Apubmed.

22. Razzoli, M., Pearson, C., Crow, S. & Bartolomucci, A. Stress, overeating, and obesity: Insights from human studies and preclinical models. *Neurosci. Biobehav. Rev.* **76**, 154–162 (2017).
23. Stephens, S. B. *et al.* The Prohormone VGF Regulates β Cell Function via Insulin Secretory Granule Biogenesis. *Cell Rep.* **20**, 2480–2489 (2017).
24. Haploinsufficiency of the autism-associated Shank3 gene leads to deficits in synaptic function, social interaction, and social communication | Molecular Autism | Full Text. https://molecularautism.biomedcentral.com/articles/10.1186/2040-2392-1-15.
25. Zhang, Z. *et al.* Release mode of large and small dense-core vesicles specified by different synaptotagmin isoforms in PC12 cells. *Mol. Biol. Cell* **22**, 2324–2336 (2011).
26. Mitchell, K. J. *et al.* Dense core secretory vesicles revealed as a dynamic Ca2+ store in neuroendocrine cells with a vesicle-associated membrane protein aequorin chimaera. *J. Cell Biol.* **155**, 41–52 (2001).
27. Bonifacino, J. S. & Glick, B. S. The mechanisms of vesicle budding and fusion. *Cell* **116**, 153–166 (2004).
28. Akinwunmi, O. A. Membrane Trafficking Mechanisms and Their Biological Relevance. *Arch. Razi Inst.* **78**, 1397–1412 (2023).
29. Alberts, B. *et al.* The Endoplasmic Reticulum. in *Molecular Biology of the Cell. 4th edition* (Garland Science, 2002).
30. Walter, P. & Johnson, A. E. Signal Sequence Recognition and Protein Targeting to the Endoplasmic Reticulum Membrane. *Annu. Rev. Cell Dev. Biol.* **10**, 87–119 (1994).
31. Alberts, B. *et al.* Transport from the ER through the Golgi Apparatus. in *Molecular Biology of the Cell. 4th edition* (Garland Science, 2002).
32. van Meer, G., Gumbiner, B. & Simons, K. The tight junction does not allow lipid molecules to diffuse from one epithelial cell to the next. *Nature* **322**, 639–641 (1986).
33. Kirchhausen, T. Adaptors for Clathrin-Mediated Traffic. *Annu. Rev. Cell Dev. Biol.* **15**, 705–732 (1999).
34. Schekman, R. & Orci, L. Coat proteins and vesicle budding. *Science* **271**, 1526–1533 (1996).
35. Duden, R. ER-to-Golgi transport: COP I and COP II function (Review). *Mol. Membr. Biol.* **20**, 197–207 (2003).
36. Barlowe, C. *et al.* COPII: A membrane coat formed by Sec proteins that drive vesicle budding from the endoplasmic reticulum. *Cell* **77**, 895–907 (1994).
37. Miller, E. A. & Barlowe, C. Regulation of coat assembly--sorting things out at the ER. *Curr. Opin. Cell Biol.* **22**, 447–453 (2010).
38. Hong, W. & Lev, S. Tethering the assembly of SNARE complexes. *Trends Cell Biol.* **24**, 35–43 (2014).
39. Malsam, J. & Söllner, T. H. Organization of SNAREs within the Golgi stack. *Cold Spring Harb. Perspect. Biol.* **3**, a005249 (2011).
40. Barlowe, C. & Helenius, A. Cargo Capture and Bulk Flow in the Early Secretory Pathway. *Annu. Rev. Cell Dev. Biol.* **32**, 197–222 (2016).
41. Arighi, E. *et al.* IdentiÆcation of Shc docking site on Ret tyrosine kinase.
42. Nickel, W. & Wieland, F. T. Biosynthetic protein transport through the early secretory pathway. *Histochem. Cell Biol.* **109**, 477–486 (1998).
43. A human homologue of the yeast HDEL receptor | Nature. https://www.nature.com/articles/348162a0.
44. The KDEL receptor: New functions for an old protein - Capitani - 2009 - FEBS Letters - Wiley Online Library. https://febs.onlinelibrary.wiley.com/doi/10.1016/j.febslet.2009.10.053.
45. Griffiths, G. & Simons, K. The trans Golgi Network: Sorting at the Exit Site of the Golgi Complex. *Science* **234**, 438–443 (1986).
46. Rambourg, A. & Clermont, Y. Three-dimensional electron microscopy: structure of the Golgi apparatus. *Eur. J. Cell Biol.* **51**, 189–200 (1990).
47. Mellman, I. & Warren, G. The Road Taken: Past and Future Foundations of Membrane Traffic. *Cell* **100**, 99–112 (2000).

48. Intracellular Functions of N-Linked Glycans | Science. https://www.science.org/doi/10.1126/science.291.5512.2364.
49. Varki, A. Biological roles of glycans. *Glycobiology* **27**, 3–49 (2017).
50. Kornfeld, S. & Mellman, I. The Biogenesis of Lysosomes. *Annu. Rev. Cell Dev. Biol.* **5**, 483–525 (1989).
51. Glick, B. S. & Nakano, A. Membrane Traffic Within the Golgi Apparatus. *Annu. Rev. Cell Dev. Biol.* **25**, 113–132 (2009).
52. Furness, J. B. & Costa, M. Types of nerves in the enteric nervous system. *Neuroscience* **5**, 1–20 (1980).
53. Rindi, G. *et al.* TNM staging of foregut (neuro)endocrine tumors: a consensus proposal including a grading system. *Virchows Arch. Int. J. Pathol.* **449**, 395–401 (2006).
54. Modlin, I. M. *et al.* Gastroenteropancreatic neuroendocrine tumours. *Lancet Oncol.* **9**, 61–72 (2008).
55. Stimulus-response coupling in neurohypophysial peptide target cells | Physiological Reviews | American Physiological Society. https://journals.physiology.org/doi/abs/10.1152/physrev.1975.55.4.489.
56. Hökfelt, T. *et al.* Neuropeptides—an overview. *Neuropharmacology* **39**, 1337–1356 (2000).
57. Eisenhofer, G. *et al.* Distinct gene expression profiles in norepinephrine- and epinephrine-producing hereditary and sporadic pheochromocytomas: activation of hypoxia-driven angiogenic pathways in von Hippel-Lindau syndrome. *Endocr. Relat. Cancer* **11**, 897–911 (2004).
58. Furlan, A. *et al.* Multipotent peripheral glial cells generate neuroendocrine cells of the adrenal medulla. *Science* **357**, eaal3753 (2017).
59. Stress-induced changes in adrenal neuropeptide Y expression are regulated by a negative feedback loop - Wang - 2013 - Journal of Neurochemistry - Wiley Online Library. https://onlinelibrary.wiley.com/doi/10.1111/jnc.12150.
60. Facilitation of transmitter action on catecholamine output by cardiac glycoside in perfused adrenal gland of guinea-pig. *Portal de Periódicos da CAPES* https://www.periodicos.capes.gov.br/index.php/acervo/buscador.html?task=detalhes&id=W2050787966.
61. Westerink, R. H. S. & Ewing, A. G. The PC12 cell as model for neurosecretion. *Acta Physiol. Oxf. Engl.* **192**, 273–285 (2008).
62. Gerdes, H. H. *et al.* The primary structure of human secretogranin II, a widespread tyrosine-sulfated secretory granule protein that exhibits low pH- and calcium-induced aggregation. *J. Biol. Chem.* **264**, 12009–12015 (1989).
63. Amano, T. *et al.* Chromosomal Dynamics at the *Shh* Locus: Limb Bud-Specific Differential Regulation of Competence and Active Transcription. *Dev. Cell* **16**, 47–57 (2009).
64. Südhof, T. C. & Rizo, J. Synaptic Vesicle Exocytosis. *Cold Spring Harb. Perspect. Biol.* **3**, a005637 (2011).
65. Walch-Solimena, C. *et al.* The t-SNAREs syntaxin 1 and SNAP-25 are present on organelles that participate in synaptic vesicle recycling. *J. Cell Biol.* **128**, 637–645 (1995).
66. Burgoyne, R. D. & Morgan, A. Secretory Granule Exocytosis. *Physiol. Rev.* **83**, 581–632 (2003).
67. Coat proteins: shaping membrane transport | Nature Reviews Molecular Cell Biology. https://www.nature.com/articles/nrm1099.
68. Edwards, R. H. Neurotransmitter release: variations on a theme. *Curr. Biol. CB* **8**, R883–885 (1998).
69. Alberts, B. *et al.* Transport from the Trans Golgi Network to the Cell Exterior: Exocytosis. in *Molecular Biology of the Cell. 4th edition* (Garland Science, 2002).
70. Vazquez-Martinez, R. & Gasman, S. The Regulated Secretory Pathway in Neuroendocrine Cells. *Front. Endocrinol.* **5**, (2014).
71. Siddhanta, A. & Shields, D. Secretory Vesicle Budding from the Trans-Golgi Network Is Mediated by Phosphatidic Acid Levels*. *J. Biol. Chem.* **273**, 17995–17998 (1998).

72. Arf1 GTPase plays roles in the protein traffic between the endoplasmic reticulum and the Golgi apparatus in tobacco and Arabidopsis cultured cells - Takeuchi - 2002 - The Plant Journal - Wiley Online Library. https://onlinelibrary.wiley.com/doi/full/10.1046/j.1365-313X.2002.01372.x?sid=nlm%3Apubmed.
73. Cancino, J., Capalbo, A. & Luini, A. Chapter 22 - Golgi-Dependent Signaling: Self-Coordination of Membrane Trafficking. in *Methods in Cell Biology* (eds. Perez, F. & Stephens, D. J.) vol. 118 359–382 (Academic Press, 2013).
74. Regulated and constitutive protein targeting can be distinguished by secretory polarity in thyroid epithelial cells. *J. Cell Biol.* **112**, 365–376 (1991).
75. Gleeson, P. A., Lock, J. G., Luke, M. R. & Stow, J. L. Domains of the TGN: Coats, Tethers and G Proteins. *Traffic* **5**, 315–326 (2004).
76. Dhara, M. *et al.* v-SNARE transmembrane domains function as catalysts for vesicle fusion. *eLife* https://elifesciences.org/articles/17571 (2016) doi:10.7554/eLife.17571.
77. Isolation of large dense-core vesicles from bovine adrenal medulla for functional studies | Scientific Reports. https://www.nature.com/articles/s41598-020-64486-3.
78. van den Pol, A. N. Neuropeptide transmission in brain circuits. *Neuron* **76**, 98–115 (2012).
79. Trueta, C. & De-Miguel, F. F. Extrasynaptic exocytosis and its mechanisms: a source of molecules mediating volume transmission in the nervous system. *Front. Physiol.* **3**, (2012).
80. Klumperman, J., Kuliawat, R., Griffith, J. M., Geuze, H. J. & Arvan, P. Mannose 6-Phosphate Receptors Are Sorted from Immature Secretory Granules via Adaptor Protein AP-1, Clathrin, and Syntaxin 6-positive Vesicles. *J. Cell Biol.* **141**, 359–371 (1998).
81. Tooze, S. A. & Huttner, W. B. Cell-free protein sorting to the regulated and constitutive secretory pathways. *Cell* **60**, 837–847 (1990).
82. Arvan, P. & Castle, D. Sorting and storage during secretory granule biogenesis: looking backward and looking forward. *Biochem. J.* **332**, 593–610 (1998).
83. SNAREs — engines for membrane fusion | Nature Reviews Molecular Cell Biology. https://www.nature.com/articles/nrm2002.
84. Borisovska, M. *et al.* v-SNAREs control exocytosis of vesicles from priming to fusion. *EMBO J.* **24**, 2114–2126 (2005).
85. Singh, N., Pathak, Z. & Kumar, H. Rab27a-mediated extracellular vesicle release drives astrocytic CSPG secretion and glial scarring in spinal cord injury. *Biomater. Adv.* **176**, 214357 (2025).
86. Fukuda, M. Distinct Rab Binding Specificity of Rim1, Rim2, Rabphilin, and Noc2: IDENTIFICATION OF A CRITICAL DETERMINANT OF Rab3A/Rab27A RECOGNITION BY Rim2*210. *J. Biol. Chem.* **278**, 15373–15380 (2003).
87. Synaptotagmin-IV modulates synaptic function and long-term potentiation by regulating BDNF release | Nature Neuroscience. https://www.nature.com/articles/nn.2315.
88. Huang, Z. & Kunes, S. Hedgehog, Transmitted along Retinal Axons, Triggers Neurogenesis in the Developing Visual Centers of the Drosophila Brain. *Cell* **86**, 411–422 (1996).
89. Tong, J. *et al.* Netrin Stimulates Tyrosine Phosphorylation of the UNC-5 Family of Netrin Receptors and Induces Shp2 Binding to the RCM Cytodomain*. *J. Biol. Chem.* **276**, 40917–40925 (2001).
90. Weiss, M., Steiner, D. F. & Philipson, L. H. Insulin Biosynthesis, Secretion, Structure, and Structure-Activity Relationships. in *Endotext* (eds. Feingold, K. R. et al.) (MDText.com, Inc., South Dartmouth (MA), 2000).
91. Synchronization of secretory protein traffic in populations of cells | Nature Methods. https://www.nature.com/articles/nmeth.1928.
92. Weigel, A. V. *et al.* ER-to-Golgi protein delivery through an interwoven, tubular network extending from ER. *Cell* **184**, 2412-2429.e16 (2021).
93. Troger, J. *et al.* Granin-derived peptides. *Prog. Neurobiol.* **154**, 37–61 (2017).

94. Secretion of a Chromaffin Granule Protein, Chromogranin, from the Adrenal Gland after Splanchnic Stimulation | Nature. https://www.nature.com/articles/215058a0.
95. Helle, K. B. The granin family of uniquely acidic proteins of the diffuse neuroendocrine system: comparative and functional aspects. *Biol. Rev.* **79**, 769–794 (2004).
96. Fricker, L. D. *et al.* Identification and Characterization of proSAAS, a Granin-Like Neuroendocrine Peptide Precursor that Inhibits Prohormone Processing. *J. Neurosci.* **20**, 639–648 (2000).
97. Chromogranins A and B and secretogranin II: evolutionary and functional aspects - Montero-Hadjadje - 2008 - Acta Physiologica - Wiley Online Library. https://onlinelibrary.wiley.com/doi/10.1111/j.1748-1716.2007.01806.x.
98. Huang, X. F. *et al.* Expressions of chromogranin A and cathepsin D in human primary hepatocellular carcinoma. *World J. Gastroenterol.* **6**, 693–698 (2000).
99. Wu, H. J., Rozansky, D. J., Parmer, R. J., Gill, B. M. & O'Connor, D. T. Structure and function of the chromogranin A gene. Clues to evolution and tissue-specific expression. *J. Biol. Chem.* **266**, 13130–13134 (1991).
100. Kirchmair, R. *et al.* The Neuropeptide Secretoneurin Acts as a Direct Angiogenic Cytokine In Vitro and In Vivo. *Circulation* **109**, 777–783 (2004).
101. The endocrine role for chromogranin A: a prohormone for peptides with regulatory properties. *Cell. Mol. Life Sci.* **64**, 2863–2886 (2007).
102. Mahata, S. K., Mahata, M., Wakade, A. R. & O'Connor, D. T. Primary Structure and Function of the Catecholamine Release Inhibitory Peptide Catestatin (Chromogranin A344−364): Identification of Amino Acid Residues Crucial for Activity. *Mol. Endocrinol.* **14**, 1525–1535 (2000).
103. D'amico, M. A., Ghinassi, B., Izzicupo, P., Manzoli, L. & Di Baldassarre, A. Biological function and clinical relevance of chromogranin A and derived peptides. *Endocr. Connect.* **3**, R45–R54 (2014).
104. Chromogranins as regulators of exocytosis - Borges - 2010 - Journal of Neurochemistry - Wiley Online Library. https://onlinelibrary.wiley.com/doi/10.1111/j.1471-4159.2010.06786.x.
105. Thakker-Varia, S. *et al.* The Neuropeptide VGF Produces Antidepressant-Like Behavioral Effects and Enhances Proliferation in the Hippocampus. *J. Neurosci.* **27**, 12156–12167 (2007).
106. Bozdagi, O. *et al.* The Neurotrophin-Inducible Gene Vgf Regulates Hippocampal Function and Behavior through a Brain-Derived Neurotrophic Factor-Dependent Mechanism. *J. Neurosci.* **28**, 9857–9869 (2008).
107. Quinn, J. P., Kandigian, S. E., Trombetta, B. A., Arnold, S. E. & Carlyle, B. C. VGF as a biomarker and therapeutic target in neurodegenerative and psychiatric diseases. *Brain Commun.* **3**, fcab261 (2021).
108. Kim, T., Tao-Cheng, J.-H., Eiden, L. E. & Loh, Y. P. Chromogranin A, an "On/Off" Switch Controlling Dense-Core Secretory Granule Biogenesis. *Cell* **106**, 499–509 (2001).
109. Lechner, T. *et al.* Chromogranin peptides in Alzheimer's disease. *Exp. Gerontol.* **39**, 101–113 (2004).
110. van Steenoven, I. *et al.* VGF Peptides in Cerebrospinal Fluid of Patients with Dementia with Lewy Bodies. *Int. J. Mol. Sci.* **20**, 4674 (2019).
111. Mahata, S. K., Mahata, M., Fung, M. & O'Connor, D. T. Catestatin: A multifunctional peptide from chromogranin A. *Regul. Pept.* **162**, 33–43 (2010).
112. Huang, E. J. & Reichardt, L. F. Neurotrophins: Roles in Neuronal Development and Function. *Annu. Rev. Neurosci.* **24**, 677–736 (2001).
113. Molecular Cloning of a Gene Sequence Regulated by Nerve Growth Factor | Science. https://www.science.org/doi/10.1126/science.3839317.
114. Kaplan, D. R. & Miller, F. D. Neurotrophin signal transduction in the nervous system. *Curr. Opin. Neurobiol.* **10**, 381–391 (2000).
115. Cattaneo, A. *et al.* Absolute Measurements of Macrophage Migration Inhibitory Factor and Interleukin-1-β mRNA Levels Accurately Predict Treatment Response in Depressed Patients. *Int. J. Neuropsychopharmacol.* **19**, pyw045 (2016).

116. Smith, K. L. *et al.* Neuropeptide S Stimulates the Hypothalamo-Pituitary-Adrenal Axis and Inhibits Food Intake. *Endocrinology* **147**, 3510–3518 (2006).
117. Bonni, A. & Greenberg, M. E. Neurotrophin regulation of gene expression. *Can. J. Neurol. Sci. J. Can. Sci. Neurol.* **24**, 272–283 (1997).
118. Neuroendocrine regulatory peptide-1 and −2: Novel bioactive peptides processed from VGF | Cellular and Molecular Life Sciences. https://link.springer.com/article/10.1007/s00018-009-8796-0.
119. Jiang, C. *et al.* Embryonic ablation of neuronal VGF increases energy expenditure and reduces body weight. *Neuropeptides* **64**, 75–83 (2017).
120. TLQP-21, a neuroendocrine VGF-derived peptide, prevents cerebellar granule cells death induced by serum and potassium deprivation - Severini - 2008 - Journal of Neurochemistry - Wiley Online Library. https://onlinelibrary.wiley.com/doi/10.1111/j.1471-4159.2007.05068.x.
121. Alder, J. *et al.* Brain-Derived Neurotrophic Factor-Induced Gene Expression Reveals Novel Actions of VGF in Hippocampal Synaptic Plasticity. *J. Neurosci.* **23**, 10800–10808 (2003).
122. Antidepressant actions of the exercise-regulated gene VGF | Nature Medicine. https://www.nature.com/articles/nm1669.
123. Stephens, S. B. *et al.* A VGF-Derived Peptide Attenuates Development of Type 2 Diabetes via Enhancement of Islet β-Cell Survival and Function. *Cell Metab.* **16**, 33–43 (2012).
124. Cocchiaro, J. L., Kumar, Y., Fischer, E. R., Hackstadt, T. & Valdivia, R. H. Cytoplasmic lipid droplets are translocated into the lumen of the Chlamydia trachomatis parasitophorous vacuole. *Proc. Natl. Acad. Sci.* **105**, 9379–9384 (2008).
125. Rossi, D. J., Jamieson, C. H. M. & Weissman, I. L. Stems Cells and the Pathways to Aging and Cancer. *Cell* **132**, 681–696 (2008).
126. Stephens, S. B. *et al.* The prohormone VGF regulates β-cell function via insulin secretory granule biogenesis. *Cell Rep.* **20**, 2480–2489 (2017).
127. Ye, Q. *et al.* Low VGF is associated with executive dysfunction in patients with major depressive disorder. *J. Psychiatr. Res.* **152**, 182–186 (2022).
128. Sahu, B. S. *et al.* Functional Genetic Variants of the Catecholamine-Release-Inhibitory Peptide Catestatin in an Indian Population: ALLELE-SPECIFIC EFFECTS ON METABOLIC TRAITS*. *J. Biol. Chem.* **287**, 43840–43852 (2012).
129. Grindheim, A. K. *et al.* Effect of Serine Phosphorylation and Ser25 Phospho-Mimicking Mutations on Nuclear Localisation and Ligand Interactions of Annexin A2. *J. Mol. Biol.* **426**, 2486–2499 (2014).
130. Song, W.-J. *et al.* Inhibitors of Lipoxygenase and Cyclooxygenase-2 Attenuate Trimethyltin-Induced Neurotoxicity through Regulating Oxidative Stress and Pro-Inflammatory Cytokines in Human Neuroblastoma SH-SY5Y Cells. *Brain Sci.* **11**, 1116 (2021).
131. Mruk, D. D. & Cheng, C. Y. Enhanced chemiluminescence (ECL) for routine immunoblotting. *Spermatogenesis* **1**, 121–122 (2011).
132. Sahu, B. S. *et al.* Catestatin regulates vesicular quanta through modulation of cholinergic and peptidergic (PACAPergic) stimulation in PC12 cells. *Cell Tissue Res.* **376**, 51–70 (2019).
133. Mukherjee, M. *et al.* Endoplasmic reticulum stress impedes regulated secretion by governing key exocytotic and granulogenic molecular switches. *J. Cell Sci.* **137**, jcs261257 (2024).
134. STED super-resolved microscopy | Nature Methods. https://www.nature.com/articles/nmeth.4593.
135. Stimulated Emission Depletion Microscopy | Chemical Reviews. https://pubs.acs.org/doi/10.1021/acs.chemrev.6b00653.
136. Breaking the diffraction resolution limit by stimulated emission: stimulated-emission-depletion fluorescence microscopy. https://opg.optica.org/ol/abstract.cfm?uri=ol-19-11-780.

137. HID-1 controls formation of large dense core vesicles by influencing cargo sorting and trans-Golgi network acidification | Molecular Biology of the Cell. https://www.molbiolcell.org/doi/10.1091/mbc.E17-08-0491?url_ver=Z39.88-2003&rfr_id=ori:rid:crossref.org&rfr_dat=cr_pub%20%200pubmed.
138. Sahu, B. S. *et al.* Role of clathrin in dense core vesicle biogenesis. *Mol. Biol. Cell* **28**, 2676 (2017).
139. Huang, A. Y., Castle, A. M., Hinton, B. T. & Castle, J. D. Resting (basal) secretion of proteins is provided by the minor regulated and constitutive-like pathways and not granule exocytosis in parotid acinar cells. *J. Biol. Chem.* **276**, 22296–22306 (2001).
140. Ohno, H. Clathrin-associated adaptor protein complexes. *J. Cell Sci.* **119**, 3719–3721 (2006).
141. Levi-Montalcini, R., Skaper, S. D., Dal Toso, R., Petrelli, L. & Leon, A. Nerve growth factor: from neurotrophin to neurokine. *Trends Neurosci.* **19**, 514–520 (1996).
142. The role of the vgf gene and VGF-derived peptides in nutrition and metabolism | Genes & Nutrition | Full Text. https://genesandnutrition.biomedcentral.com/articles/10.1007/s12263-007-0047-0.
143. Urolithin A induces mitophagy and prolongs lifespan in C. elegans and increases muscle function in rodents | Nature Medicine. https://www.nature.com/articles/nm.4132.
144. Tyrosine hydroxylase phosphorylation: regulation and consequences - Dunkley - 2004 - Journal of Neurochemistry - Wiley Online Library. https://onlinelibrary.wiley.com/doi/10.1111/j.1471-4159.2004.02797.x.
145. Dominguez, N., van Weering, J. R. T., Borges, R., Toonen, R. F. G. & Verhage, M. Dense-core vesicle biogenesis and exocytosis in neurons lacking chromogranins A and B. *J. Neurochem.* **144**, 241–254 (2018).
146. Gerdes, H.-H. & Glombik, M. M. Signal-mediated sorting to the regulated pathway of protein secretion. *Ann. Anat. - Anat. Anz.* **181**, 447–453 (1999).
147. Lancaster, G. I. *et al.* Evidence that TLR4 Is Not a Receptor for Saturated Fatty Acids but Mediates Lipid-Induced Inflammation by Reprogramming Macrophage Metabolism. *Cell Metab.* **27**, 1096-1110.e5 (2018).
148. Functional proteomic screens reveal an essential extracellular role for hsp90α in cancer cell invasiveness | Nature Cell Biology. https://www.nature.com/articles/ncb1131.
149. Spatial and temporal coordination of insulin granule exocytosis in intact human pancreatic islets | Diabetologia. https://link.springer.com/article/10.1007/s00125-015-3747-9.
150. Moro, A., Hoogstraaten, R. I., Persoon, C. M., Verhage, M. & Toonen, R. F. Quantitative analysis of dense-core vesicle fusion in rodent CNS neurons. *STAR Protoc.* **2**, 100325 (2021).
151. Current molecular approaches to investigate pre-synaptic dysfunction - Harper - 2021 - Journal of Neurochemistry - Wiley Online Library. https://onlinelibrary.wiley.com/doi/10.1111/jnc.15316.
152. Baginska, U., Balagura, G., Toonen, R. F. & Verhage, M. High-throughput assay for regulated secretion of neuropeptides in mouse and human neurons. *J. Biol. Chem.* **300**, 107321 (2024).
153. Mechanisms of Exocytosis in Insulin-Secreting B-Cells and Glucagon-Secreting A-Cells - Barg - 2003 - Pharmacology & Toxicology - Wiley Online Library. https://onlinelibrary.wiley.com/doi/full/10.1034/j.1600-0773.2003.920102.x.
154. Li, Y. & Tsien, R. W. pHTomato: A genetically-encoded indicator that enables multiplex interrogation of synaptic activity. *Nat. Neurosci.* **15**, 1047–1053 (2012).
155. Visualizing secretion and synaptic transmission with pH-sensitive green fluorescent proteins | Nature. https://www.nature.com/articles/BF28190.
156. A small GTP-binding protein dissociates from synaptic vesicles during exocytosis | Nature. https://www.nature.com/articles/349079a0.
157. Tronche, F., Kellendonk, C., Reichardt, H. M. & Schütz, G. Genetic dissection of glucocorticoid receptor function in mice. *Curr. Opin. Genet. Dev.* **8**, 532–538 (1998).

158. Kwon, S. E. & Chapman, E. R. Synaptophysin Regulates the Kinetics of Synaptic Vesicle Endocytosis in Central Neurons. *Neuron* **70**, 847–854 (2011).
159. Nakata, T. & Hirokawa, N. Microtubules provide directional cues for polarized axonal transport through interaction with kinesin motor head. *J. Cell Biol.* **162**, 1045–1055 (2003).
160. Lewis, J. E. The role of VGF and its derived peptides in the regulation of energy.
161. Wu, L.-G., Hamid, E., Shin, W. & Chiang, H.-C. Exocytosis and Endocytosis: Modes, Functions, and Coupling Mechanisms*. *Annu. Rev. Physiol.* **76**, 301–331 (2014).
162. Fulop, T., Radabaugh, S. & Smith, C. Activity-Dependent Differential Transmitter Release in Mouse Adrenal Chromaffin Cells. *J. Neurosci.* **25**, 7324–7332 (2005).
163. Clayton, E. L., Evans, G. J. O. & Cousin, M. A. Bulk Synaptic Vesicle Endocytosis Is Rapidly Triggered during Strong Stimulation. *J. Neurosci.* **28**, 6627–6632 (2008).
164. Retrograde transport from endosomes to the trans-Golgi network | Nature Reviews Molecular Cell Biology. https://www.nature.com/articles/nrm1985.
165. Tooze, S. A., Abada, A. & Elazar, Z. Endocytosis and Autophagy: Exploitation or Cooperation? *Cold Spring Harb. Perspect. Biol.* **6**, a018358 (2014).
166. Mahata, S. K., Mahata, M., Parmer, R. J. & O'Connor, D. T. Desensitization of Catecholamine Release: THE NOVEL CATECHOLAMINE RELEASE-INHIBITORY PEPTIDE CATESTATIN (CHROMOGRANIN A344–364) ACTS AT THE RECEPTOR TO PREVENT NICOTINIC CHOLINERGIC TOLERANCE*. *J. Biol. Chem.* **274**, 2920–2928 (1999).
167. Fassio, A. *et al.* Emerging Role of the Autophagy/Lysosomal Degradative Pathway in Neurodevelopmental Disorders With Epilepsy. *Front. Cell. Neurosci.* **14**, 39 (2020).